ORIGINAL RESEARCH

Crk and *Crkl* Are Required in the Endocardial Lineage for Heart Valve Development

Bingruo Wu, MD, MMed, MS*; Brian Wu, MD*; Sonia Benkaci, MSc; Lijie Shi ⬙, PhD; Pengfei Lu ⬙, PhD; Taeju Park, PhD; Bernice E. Morrow ⬙, PhD; Yidong Wang ⬙, PhD; Bin Zhou ⬙, MD, PhD

BACKGROUND: Endocardial cells are a major progenitor population that gives rise to heart valves through endocardial cushion formation by endocardial to mesenchymal transformation and the subsequent endocardial cushion remodeling. Genetic variants that affect these developmental processes can lead to congenital heart valve defects. *Crk* and *Crkl* are ubiquitously expressed genes encoding cytoplasmic adaptors essential for cell signaling. This study aims to explore the specific role of *Crk* and *Crkl* in the endocardial lineage during heart valve development.

METHODS AND RESULTS: We deleted *Crk* and *Crkl* specifically in the endocardial lineage. The resultant heart valve morphology was evaluated by histological analysis, and the underlying cellular and molecular mechanisms were investigated by immunostaining and quantitative reverse transcription polymerase chain reaction. We found that the targeted deletion of *Crk* and *Crkl* impeded the remodeling of endocardial cushions at the atrioventricular canal into the atrioventricular valves. We showed that apoptosis was temporally increased in the remodeling atrioventricular endocardial cushions, and this developmentally upregulated apoptosis was repressed by deletion of *Crk* and *Crkl*. Loss of *Crk* and *Crkl* also resulted in altered extracellular matrix production and organization in the remodeling atrioventricular endocardial cushions. These morphogenic defects were associated with altered expression of genes in BMP (bone morphogenetic protein), connective tissue growth factor, and WNT signaling pathways, and reduced extracellular signal-regulated kinase signaling activities.

CONCLUSIONS: Our findings support that *Crk* and *Crkl* have shared functions in the endocardial lineage that critically regulate atrioventricular valve development; together, they likely coordinate the morphogenic signals involved in the remodeling of the atrioventricular endocardial cushions.

Key Words: *Crk* ∎ *Crkl* ∎ endocardial cushion ∎ endocardium ∎ heart valve development

Congenital heart disease affects ~1% of all live births,[1,2] and malformation of the heart valves accounts for 20% to 30% of all congenital heart disease.[3] Congenital heart disease, including heart valve defects, often requires surgical interventions for survival and remains the leading cause of infant death.[4,5] In later life, congenital heart valve defects can increase the risk of developing cardiac complications, leading to heart failure.[6,7] Studies using human genetics, functional genomics, and animal models have made significant progress in understanding the cause of congenital heart valve malformation through identifying genetic and environmental risk factors.[5,8] However, the underlying molecular and cellular changes remain

<div style="border: 2px solid red;">

RESEARCH PERSPECTIVE

What Is New?

- This study reveals that *Crk/Crkl* in the endocardial lineage critically regulates cell apoptosis and extracellular matrix arrangement essential for the remodeling of atrioventricular endocardial cushions during valvulogenesis.

What Question Should Be Addressed Next?

- Future studies are needed to determine the molecular signaling mechanism by which *Crk/Crkl* controls endocardial cushion remodeling and identify the protein partners of *Crk/Crkl* in the signaling pathways regulated by *Crk/Crkl*.

</div>

<div style="border: 2px solid red;">

Nonstandard Abbreviations and Acronyms

EdU	5-ethynyl-2′-deoxyuridine
ERK	extracellular signal-regulated kinase
AVC	atrioventricular canal
DKO	double knockout
ECM	extracellular matrix
EndMT	endocardial-to-mesenchymal transformation
OFT	outflow tract
RT-qPCR	real-time quantitative polymerase chain reaction
TUNEL	terminal deoxynucleotidyl transferase dUTP nick end labeling

</div>

incompletely understood. Better understanding of normal mammalian heart valve formation will help to elucidate these changes in the pathogenesis of congenital heart valve defects caused by genetic mutations and environmental insults.

In mice, formation of the heart valves starts at embryonic day 9.5 when the heart looping is completed. A subpopulation of endocardial cells at the atrioventricular canal (AVC) undergoes endocardial-to-mesenchymal transformation (EndMT) and becomes mesenchymal cells that invade the swollen and matrix-rich subendocardial spaces named endocardial cushions.[9–11] EndMT ceases around embryonic day 11.5, when endocardial cushions are fully cellularized and begin to function as valve primordia. The valve primordia subsequently undergo a complex of morphogenic changes to form the valve leaflets. This process is named post-EndMT remodeling, which involves cell proliferation, apoptosis, and organized extracellular matrix (ECM) production. The post-EndMT remodeling of endocardial cushions

is spatiotemporally regulated by the multiple molecular signals from the cushion endocardium to the newly formed valve mesenchyme.[12,13] Therefore, the endocardial cells at AVC are not only the major progenitor cell source giving rise to the mesenchyme of the atrioventricular valves but also a main signaling source directing the remodeling process that sculpts the endocardial cushions into the functional valve leaflets.[3,14] Uncovering the endocardial signaling modulators critical for the valve remodeling is thus important to reveal disease mechanisms of congenital heart valve defects.

Crk and *Crkl* (*Crk*-like) belong to the *Crk* gene family that encodes major cellular adaptor proteins containing the SRC homology 2 and 3 domains.[15–17] *Crk* and *Crkl* interact with >40 cellular proteins through SH2 and SH3 domains.[18] They mediate tyrosine kinase signals such as mitogen-activated protein kinase, which are involved in a number of biological processes including cell proliferation, apoptosis, adhesion, and migration.[18] Mutations in *Crk* and *Crkl* are associated with several human diseases.[19–24] Importantly, *Crkl* is localized to 22q11.2, which is hemizygously deleted in the 22q11.2 deletion syndrome (22q11.2DS), and ~70% of patients with 22q11.2DS develop congenital heart disease affecting the cardiac outflow tract (OFT).[16] In mice, germline loss of *Crkl* results in similar cardiovascular defects affecting the cardiac OFT.[25,26] Our previous mouse studies further showed that *Crkl* genetically interacts with *Tbx1*, a key 22q11.21 gene, and plays a dosage-dependent role in OFT development.[23,27] Like *Crkl*, germline loss of *Crk* in mice also causes cardiovascular defects.[28] On the other hand, *Crk* and *Crkl* express ubiquitously during embryogenesis and function redundantly in mediating molecular signals such as the Reelin signaling,[29] and our recent mouse studies indicated that *Crk* and *Crkl* have shared functions in the cardiac neural crest cells for the cardiac OFT septation by regulating vascular smooth muscle differentiation and apoptosis, possibly through the Notch and integrin signaling.[30]

These observations promoted us to investigate the potential shared functions of *Crk* and *Crkl* in the endocardial cells during heart valve development as they are a major progenitor population of the heart valves giving rise to valve mesenchymal cells. We deleted *Crk* and *Crkl* in the endocardial cells and their progenies using an endocardial cell specific Cre line, *Nfatc1Cre*, which was generated in our laboratory by inserting an IRES-Cre cassette at the 3′ untranslated region of *Nfatc1*.[31] We found that deletion of all 4 alleles, that is, both of *Crk* and *Crkl*, is embryonic lethal and causes severe defects in the developing atrioventricular valves. We showed that the valve structural defects are preceded by decreased cell apoptosis and altered ECM when the atrioventricular endocardial cushions undergo the post-EndMT remodeling. We also found downregulation of several genes in the BMP (bone morphogenetic

protein), connective tissue growth factor, or WNT signaling pathway involved in tissue morphogenesis. These findings support a shared function between *Crk* and *Crkl* in the endocardial lineage that regulates the remodeling of endocardial cushions essential for the formation of the atrioventricular valves, likely by coordinating tissue morphogenic signals.

METHODS

Data Availability

The data supporting this study's findings are available from the corresponding author upon reasonable request.

Mice

Mouse housing and experiments were performed according to the protocol approved by the Institutional Animal Care and Use Committee of Albert Einstein College of Medicine. Both *Nfatc1*Cre [31] and floxed *Crk* and *Crkl* mice[29] were backcrossed to the C57BL/6J inbred mice (Jackson Laboratory, Stock Number: 000664) for >10 generations before being used for this study. The *Nfatc1*Cre mice then were crossed with the floxed *Crk* and *Crkl* mice to generate the endocardial lineage-specific *Crk* and *Crkl* double knockout (DKO) mice. Adult mice or mouse embryos were genotyped by polymerase chain reaction using genomic DNA from the tail and yolk sac, respectively. Noontime on the day of detecting vaginal plugs was designated as embryonic day 0.5. Pregnant female mice were euthanized by isoflurane in a sealed container.

Histology

Mouse embryos from embryonic day 12.5 to embryonic day 14.5 were isolated in PBS and fixed in 4% paraformaldehyde overnight at 4 °C. The samples were then dehydrated through an ethanol gradient, treated with xylene, and embedded in paraffin wax. Serial sections of whole heart were obtained using a Leica microtome and subjected to hematoxylin and eosin or Alcian blue staining following the standard protocols. The stained tissues were imaged using a Zeiss Axioskop 2 plus microscope. The length/width ratio of the valve leaflet was quantified using Image J, and the hearts from 4 embryos of each genotype were analyzed.

Immunofluorescence

The tissue sections from embryonic day 10.5 to embryonic day 16.5 embryos, prepared as described above, were antigen retrieved by boiling in 10 mM of sodium citrate (pH 6.0) and blocked with 5% normal horse serum before being incubated with primary and secondary antibodies (Table S1). The immunostained tissues were visualized and photographed using a Leica DMi8 confocal microscope.

RNAscope In Situ Hybridization

Embryos at embryonic day 11.5 were isolated in PBS and fixed in 4% paraformaldehyde for at least 24 hours and processed for frozen embedding in the optimal cutting temperature (OCT) compound. The tissues were processed for RNAscope analysis following the manufactural protocol for the fixed frozen tissues using the RNAscope 2.5 HD Detection Reagent-Red Kit (ACDBio). After the RNAscope analysis, the tissues were costained for vascular endothelial–cadherin antibodies to mark the endocardial cells. The stained tissues were imaged using a Leica DMi8 confocal microscope.

Proliferation Assay

Cell proliferation was examined by the 5-ethynyl-2′-deoxyuridine (EdU; Life Technology) assay and immunostaining for the phospho-histone H3. For the EdU assay, the pregnant female mice at embryonic day 13.5 were injected with EdU through intraperitoneal injection with a dosage of 10 mg/kg. After a 2-hour pulse, embryos were collected and processed for the frozen sections. Briefly, embryonic day 13.5 embryos were fixed in 4% paraformaldehyde at 4 °C for 1 hour, incubated in 15% and 30% sucrose sequentially and embedded in OCT compounds. The 8-μm tissue sections were obtained and post-fixed in the cold ethanol and acetone (1:1) solution for 5 minutes and stored at −80 °C. Tissue sections were air dried for 45 minutes before staining. The EdU incorporation was detected using the EdU Imaging Kit (Life Technology; C10337) and counterstained with DAPI (Vector Laboratories). The stained sections were photographed using a Leica DMi8 confocal microscope. Positive EdU labeling was quantified for the endocardial lineage marked by green fluorescent protein expression within AVC cushions using Image J software, and the data were presented as the percentage of EdU-positive cells. Three individual hearts were analyzed for each genotype and subjected to the statistical calculation. Immunostaining of phospho-histone H3 was performed on the paraffin sections, and SOX9 was costained to mark the valve mesenchymal cells. The phospho-histone H3 positive cells within AVC cushions marked by SOX9 staining were quantified by dividing the total cell number with cushion area.

Apoptosis Assay

Cell apoptosis was examined by the terminal deoxynucleotidyl transferase dUTP nick end labeling (TUNEL) assay and immunostaining for cleaved Caspase3. Frozen sections from embryonic day 10.5 to embryonic day 16.5 embryos were prepared as described above

for the EdU assay. The apoptotic cells were detected using the Dead End Fluorometric TUNEL System (Promega) and counterstained with DAPI. Costaining for Slug was performed to mark the mesenchymal cells. The stained sections were photographed using a Leica DMI8 confocal microscope. The quantification of TUNEL assays was carried out in Image J. The numbers of TUNEL-positive cells were counted, and the density was obtained by counting the number of positive staining cells in the entire cushion area from the serial sections for the forming mitral valve and tricuspid valve. Three samples were used for each embryonic stage from embryonic day 10.5 to embryonic day 16.5.

RNA Extraction and Real-Time Quantitative Polymerase Chain Reaction

The hearts were isolated from embryonic day 13.5 embryos, and the atrioventricular valve tissues were micro-dissected for the total RNA extraction using Trizol (Invitrogen). First strand cDNA was synthesized using the Superscript IV Reverse Transcriptase Kit (Invitrogen). Real-time quantitative polymerase chain reaction (RT-qPCR) was performed using the Power SYBR Green PCR Master Mix (ABI). Gene-specific primers (Table S2) were used for quantitative polymerase chain reaction. The expression of $Tf2b$ was used as an internal control. The expression of genes was calculated using the $2^{-\Delta\Delta CT}$ method. Four biological repeats were performed, and each consisted of 3 pooled samples from individual hearts for each genotype. The mean relative expression of each gene between groups was used for statistically significant analysis.

Statistical Analysis

The graphs were plotted with mean and standard errors using Prism 8 (GraphPad Software). Two-tailed unpaired t tests were used for statistical comparison between the 2 groups. One-way ANOVA was used for statistical comparison among ≥3 groups.

RESULTS

Crk and Crkl in the Endocardial Lineage Is Required for Embryonic Survival

Deletion of Crk or $Crkl$ in the endocardial lineage using $Nfatc1^{Cre}$[29,31] does not result in obvious heart defects, and the individual conditional null mutants survived to birth, suggesting that they have shared functions in the endocardial lineage during embryonic heart development. To test this hypothesis, we generated endocardial DKO mice using $Nfatc1^{Cre}$ and the compound floxed Crk and $Crkl$ mice ($Crk^{f/f}$; $Crkl^{f/f}$).[30] We confirmed the efficiency and specificity of deletion by immunostaining for CRK and by RNAscope in situ hybridization (ISH) for $Crkl$.

The results showed that, while both genes are expressed ubiquitously in embryonic day 11.5 hearts of control embryos ($Crk^{f/f}$; $Crkl^{f/f}$), the DKO embryos have reduced expression of both genes in the mesenchymal cushions at AVC and the proximal OFT derived from the endocardial cells (Figure 1A through 1C and Figure S1). We then examined the embryos collected at multiple developmental stages from embryonic day 10.5 to embryonic day 17.5. We found that 6 of 10 of the DKO embryos at embryonic day 14.5 had developed subepidermal edema (indicative of heart failure; Figure 1D), 4 of 14 of the DKO embryos inspected at embryonic day 15.5 were already dead and necrotic (Figure 1E). At embryonic day 16.5 or embryonic day 17.5, all 11 DKO embryos inspected were dead and runted. These findings suggest that Crk and $Crkl$ play shared roles in the endocardial lineage of the developing heart that is necessary for embryonic survival.

Endocardial Crk and Crkl Regulate Remodeling of Atrioventricular Endocardial Cushion

Heart valve development begins with endocardial cushion formation through EndMT between embryonic day 9.5 and embryonic day 10.5 in mice. Endocardial cushions then continue growing and remodeling to form the thin valve leaflets at birth. We examined the heart morphology between embryonic day 10.5 and embryonic day 14.5 by hematoxylin and eosin staining to explore the potential roles of Crk and $Crkl$ in EndMT and post-EMT cushion remodeling. We found that the endocardial cushions at AVC are comparable between control and DKO embryos at embryonic day 10.5 (Figure S2) and embryonic day 12.5 (Figure 2A), suggesting that the deletion does not affect EndMT and initial cellularization of the AVC endocardial cushions. In contrast, further development of the AVC endocardial cushions into the atrioventricular valves (ie, the remodeling of the endocardial cushions) in the DKO embryos is delayed at embryonic day 13.5. This is evidenced by their primitive appearance compared with the normal remodeling valves in the control embryos that begin to display the discrete mitral and tricuspid valves (Figure 2B). By embryonic day 14.5, both atrioventricular valves elongate significantly in the control embryos to form the valve leaflets, but they remain blunted in the DKO embryos, as shown by the reduced length to width ratio of the valve leaflets (Figure 2C through 2E). Of note, the remodeling defect is restricted to the atrioventricular valves, as we did not find obvious morphological changes in the semilunar valves (Figures S3 and S4). In addition, 4 of 5 embryonic day 14.5 DKO embryos examined by hematoxylin and eosin staining appear to have an atrioventricular septal defect when compared with 5 littermate controls that have normal developing atrioventricular septa (Figure 2C and 2E). In contrast, no apparent
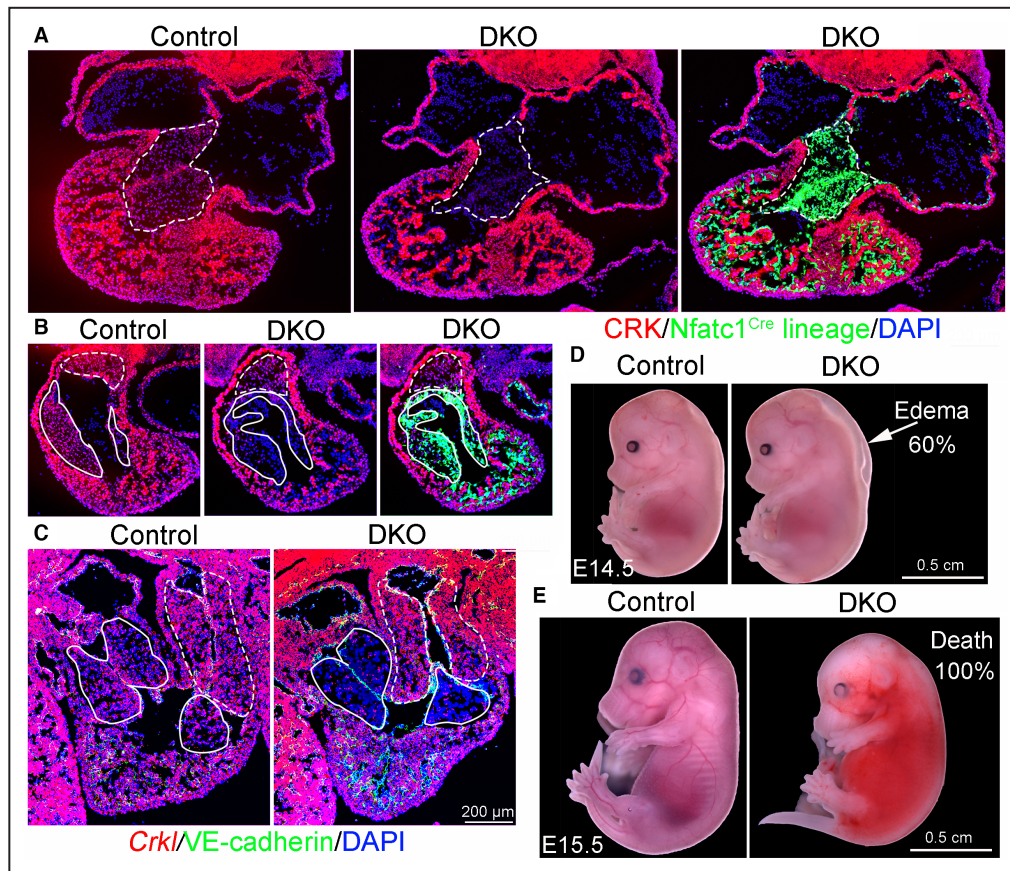
Figure 1. Deletion of *Crk* and *Crkl* in the endocardial lineage is embryonic lethal.
A and **B**, Immunostaining shows the expression of *Crk* in embryonic day 11.5 control and *Crk* and *Crkl* DKO embryos (*Crk$^{f/f}$*; *Crkl$^{f/f}$*; *R26$^{fsGFP/+}$*; *Nfatc1^{Cre}*; DKO). Note that the DKO heart has diminished expression of *Crk* in the endocardial cushions at AVC (**A**, labeled by green fluorescent protein and outlined by dashed lines) and the proximal OFT cushions (**B**, marked by the solid line; the dash line indicates the NCC-derived distal OFT cushions). **C**, RNAscope in situ hybridization shows the expression of *Crkl* (red) is diminished in the endocardial cushions at AVC and proximal OFT outlined by the solid and dash lines, respectively. Coimmunostaining for cadherin-5 (green) shows the endocardial layer. **D** and **E**, Whole embryo views show that DKO embryos have the subcutaneous edema (arrow) at embryonic day 14.5 (**D**); they are runted and absorbed at embryonic day 15.5 (**E**). AVC indicates atrioventricular canal; DKO, double knockout; NCC, neural crest cell; and OFT, outflow tract.

difference of myocardial development was observed between control and DKO embryos at embryonic day 14.5 (Figure S5). Because the DKO embryos died between embryonic day 15.5 and embryonic day 16.5, we were unable to carry out any meaningful histological studies to characterize the cardiac morphology at the later stages. These findings support that *Crk* and *Crkl* have shared functions in the endocardial lineage essential for the remodeling of the AVC endocardial cushions into the atrioventricular valves.

Endocardial *Crk* and *Crkl* Regulates Apoptosis During AVC Endocardial Cushion Remodeling

Spatiotemporally regulated cell apoptosis drives the remodeling of endocardial cushions to form the elongated heart valves. To better reveal the role of programmed cell death in the formation of the atrioventricular valves, we performed TUNEL assays to assess the cell apoptosis at the AVC endocardial cushions from embryonic day 10.5 to embryonic day 16.5 that covers the initial cellularized endocardial cushions by EndMT to subsequent remodeling of the cushions into the thin valve leaflets. The results showed that few apoptotic cells are present in the AVC endocardial cushions before embryonic day 12.5, but intensive cell apoptosis takes place between embryonic day 12.5 and embryonic day 13.5 when the fully cellularized endocardial cushions begin to transform into the elongated valve leaflets (Figure 3). After embryonic day 13.5, the number of apoptotic cells in the remodeling mitral and tricuspid valves is markedly reduced and remained at a low level until embryonic day 16.5. These results suggest that
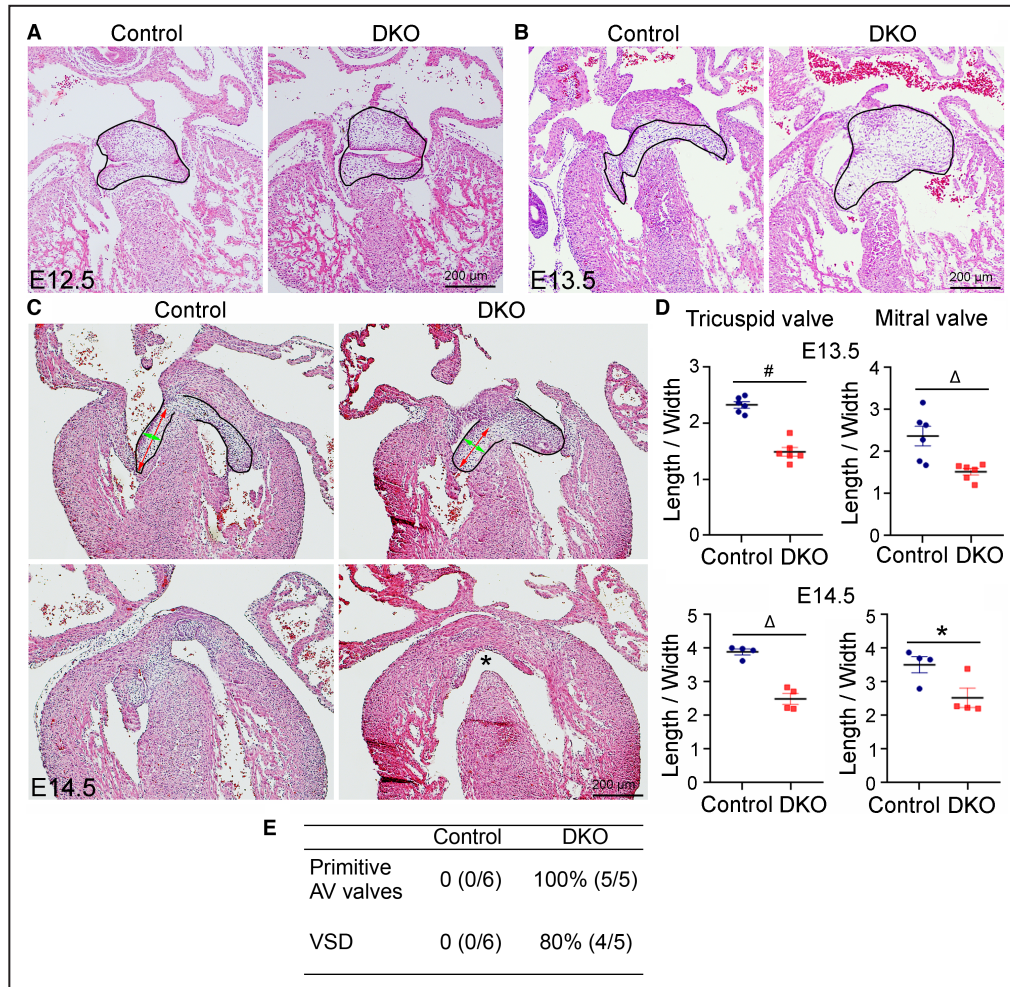
Figure 2. Loss of endocardial *Crk* and *Crkl* causes defective atrioventricular valves and atrioventricular septum.
A through **C**, Representative images of hematoxylin and eosin staining for embryonic day 12.5, embryonic day 13.5, and embryonic day 14.5 hearts show a progressive morphogenic change leading to underdeveloped atrioventricular valves (outlined by the solid line) and defective atrioventricular septum (indicated by asterisk) in DKO embryos. **D**, Bar graphs show the significant difference in the length/ width ratio of the tricuspid or mitral valve at embryonic day 13.5 (n=6/group) and embryonic day 14.5 (n=4/group). The red and green double-sided arrows in **C** represent the length and width of the valve leaflet, respectively. $*P<0.05$; $^{\Delta}P<0.01$; $^{\#}P<0.01$ by the unpaired Student's t test. **E**, A table summarizing the penetrance of the valve defect and defective atrioventricular septum observed in embryonic day 14.5 DKO embryos. AV indicates atrioventricular; DKO, double knockout; and VSD, ventricular septal defect.

apoptosis is essential to initiate valve remodeling between embryonic day 12.5 and embryonic day 13.5.

To determine whether loss of *Crk* and *Crkl* affected cell apoptosis, we then performed TUNEL assays on heart sections from embryonic day 13.5 control and DKO embryos. The results revealed a markedly reduced number of apoptotic cells in the remodeling endocardial cushions at the AVC of embryonic day 13.5 DKO embryos when compared with that in the control littermates (Figure 4A and 4B). Consistently, immunostaining for the activated caspase 3 showed that the DKO embryos had significantly reduced cleaved caspase 3 activities in the AVC endocardial cushions when compared with the

control embryos at embryonic day 13.5 (Figure 4C and 4D). We also examined mRNA expression of the apoptotic genes in the AVC endocardial cushions isolated from embryonic day 13.5 hearts by RT-qPCR and found that the DKO embryos had significantly reduced expression of *Casp3* and *Bax* in the AVC endocardial cushions (Figure 4E). In addition, we examined cell proliferation by the EdU labeling of cells in the S-phase of the active cell cycle as well as immunostaining for phospho-histone H3 for cells in the M-phase. The results from both assays showed that cell proliferation in the remodeling endocardial cushions at AVC is not affected in embryonic day 13.5 DKO embryos (Figure S6). Collectively, these
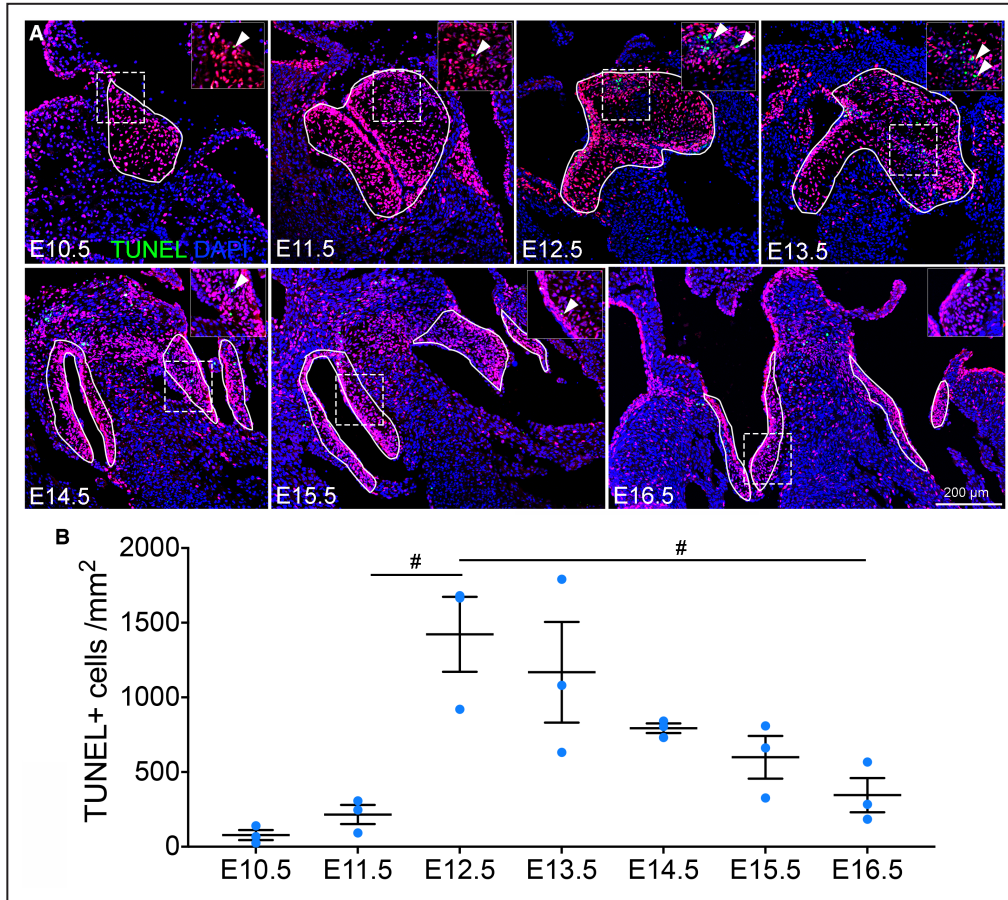
Figure 3. Spatiotemporally regulated programmed cell death in the developing atrioventricular valves.

A, Representative images of TUNEL assay showing the apoptotic cells (green) in the developing atrioventricular valves (outlined by solid lines) of wild-type embryos at the stages from embryonic day 10.5 to embryonic day 16.5. The valve mesenchymal cells were marked by coimmunostaining for SLUG (red). The insets show the higher magnification of the boxed region outlined by dashed lines. **B**, A bar graph showing the quantification of the average density of the apoptotic cells in the forming atrioventricular valves. n=3/group, #$P<0.01$ by ANOVA test. TUNEL indicates terminal deoxynucleotidyl transferase dUTP nick end labeling.

observations support that the reduced programmed cell death may contribute to the blunted atrioventricular valve leaflets in the DKO hearts, as apoptosis is necessary to sculpture the endocardial cushions into the valve leaflets.

Endocardial *Crk* and *Crkl* Regulates ECM During AVC Endocardial Cushion Remodeling

The ECM synthesis and organized deposition, in addition to cell proliferation and apoptosis, are part of the remodeling process essential for transforming the endocardial cushions into the heart valves. To better reveal the developmental changes in the organized ECM deposition or ECM fibrous alignment in the forming atrioventricular valves, we examined the expression of collagen and elastin in the AVC endocardial cushions

between embryonic day 10.5 (ie, active EndMT) and embryonic day 16.5 (ie, the formation of the valve leaflets). The results showed weak collagen I presence at AVC at embryonic day 10.5 and embryonic day 11.5 during the cellularization of the AVC endocardial cushions by EndMT. Beginning at embryonic day 12.5, its expression in the cushion mesenchyme becomes prominent, and the expression persists at a high level from embryonic day 13.5 to embryonic day 16.5 (Figure 5A). Similarly, elastin is expressed at a high level in the mesenchymal cells after embryonic day 13.5, but its expression is absent in these cells before embryonic day 13.5 (Figure 5B).

To explore whether loss of *Crk* and *Crkl* affected ECM deposition, we then examined the production of the major ECM components (proteoglycans, collagens, and elastin) in the remodeling atrioventricular valves
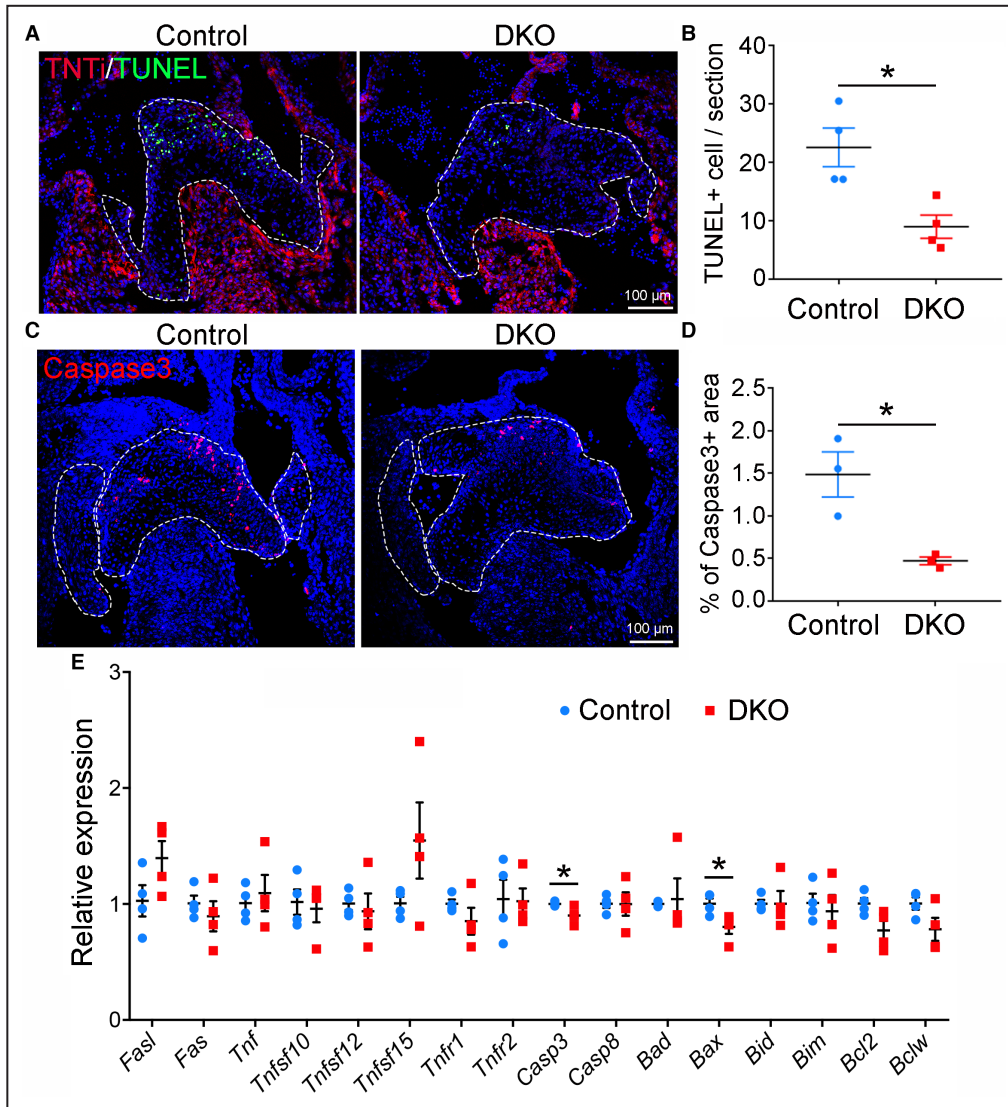
Figure 4. Loss of endocardial *Crk* and *Crkl* inhibits programmed cell death.
A, Representative images of TUNEL assay showing reduced TUNEL-labeled apoptotic cells (green) in the AVC endocardial cushions (outlined by dashed lines) of embryonic day 13.5 DKO embryos. Coimmunostaining for TNNI (red) marks the cardiomyocytes. **B**, A bar graph showing the quantification result of the number of the apoptotic cells. n=4/group. **C**, Representative images of immunostaining showing the reduced expression of cleaved caspase 3 in the AVC endocardial cushions (outlined by dashed lines) of embryonic day 13.5 DKO embryos. **D**, A bar graph showing the quantification result of the caspase 3 staining. n=3/group. **E**, RT-qPCR analysis of gene expression in the atrioventricular valve tissues from embryonic day 13.5 control and DKO embryos. n=4/group. Unpaired Student's *t* test was used for the statistical calculation. *$P<0.05$. AVC indicates atrioventricular canal; DKO, double knockout; RT-qPCR, real-time quantitative polymerase chain reaction; and TUNEL, terminal deoxynucleotidyl transferase dUTP nick end labeling.

isolated from embryonic day 13.5 hearts by RT-qPCR. We found that the expression of *Acan*, encoding for a major proteoglycan Aggrecan, is significantly downregulated in the DKO atrioventricular valves when compared with the control valves, whereas the expression of other proteoglycan genes, *Vcan*, *Habp2*, and *Hapln1*, is not affected (Figure 6A). In addition, Alcian blue staining and

immunostaining for *Vcan* and *Habp2* showed that proteoglycan deposition is not affected in the DKO atrioventricular valves (Figure S7). On the other hand, the results of RT-qPCR showed that the expression of several collagen genes (*Col1a1*, *Col1a2*, *Col3a1* and *col11a1*) and elastin (*Eln*) is significantly decreased in the DKO atrioventricular valves (Figure 6A). We confirmed the expression
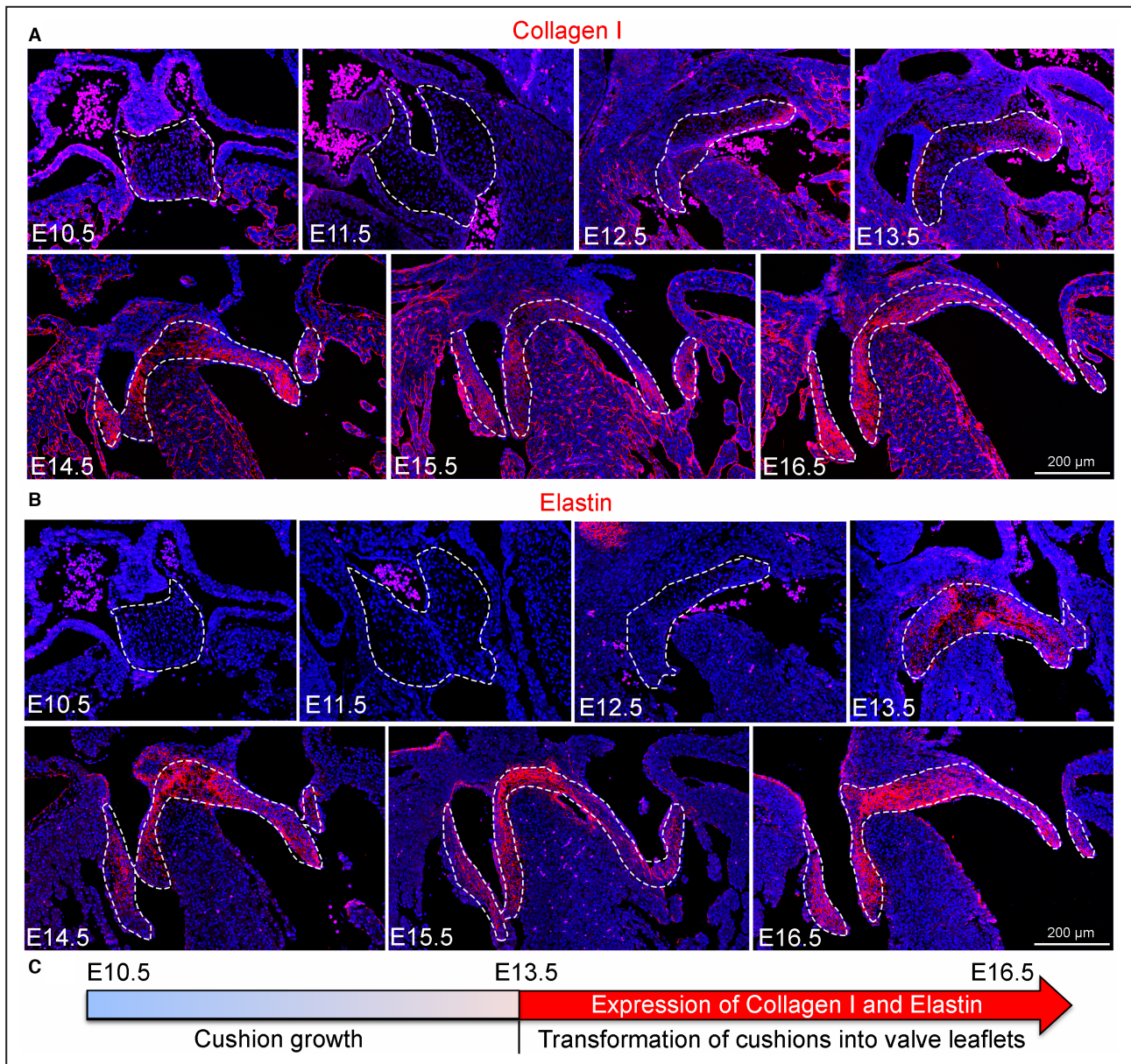
Figure 5. Spatiotemporally regulated synthesis and deposition of collagen I and elastin in the developing atrioventricular valves.

A and B, Representative immunostaining images showing increased synthesis and deposition of collagen I (**A**) and elastin (**B**) in the developing wild-type atrioventricular valves. Note that collagen I is weakly in the AVC endocardial cushions between embryonic day 10.5 and embryonic day 11.5, and its expression is upregulated from embryonic day 12.5 in the remodeling atrioventricular endocardial cushions and valves. Elastin is not expressed in either endocardial or mesenchymal cells before embryonic day 13.5, but it is expressed at a high level in the atrioventricular valve mesenchyme from embryonic day 13.5 to embryonic day 16.5. **C**, Summary of the expression of collagen I and elastin during early valve (cushion) growth (embryonic day 10.5 to embryonic day E13.5) and late valve remodeling (transformation of endocardial cushions into the valve leaflets [embryonic day 13.5 to embryonic day 16.5]). AVC indicates atrioventricular canal; and E, embryonic day.

changes at the protein levels by immunostaining for collagen I and elastin, 2 major ECM components in the remodeling atrioventricular valves (Figure 6B through 6E). Significantly, we found that collagen and elastin form distinct fibrous networks in the remodeling atrioventricular valves of embryonic day 13.5 control embryos, but the fibrous networks appear to be disorganized in the DKO embryos (Figure 6B and 6C). These findings demonstrate that *Crk* and *Crkl* are required for the developmentally regulated ECM synthesis and organized ECM deposition in the remodeling atrioventricular valves to acquire the delicate leaflet structure and function.
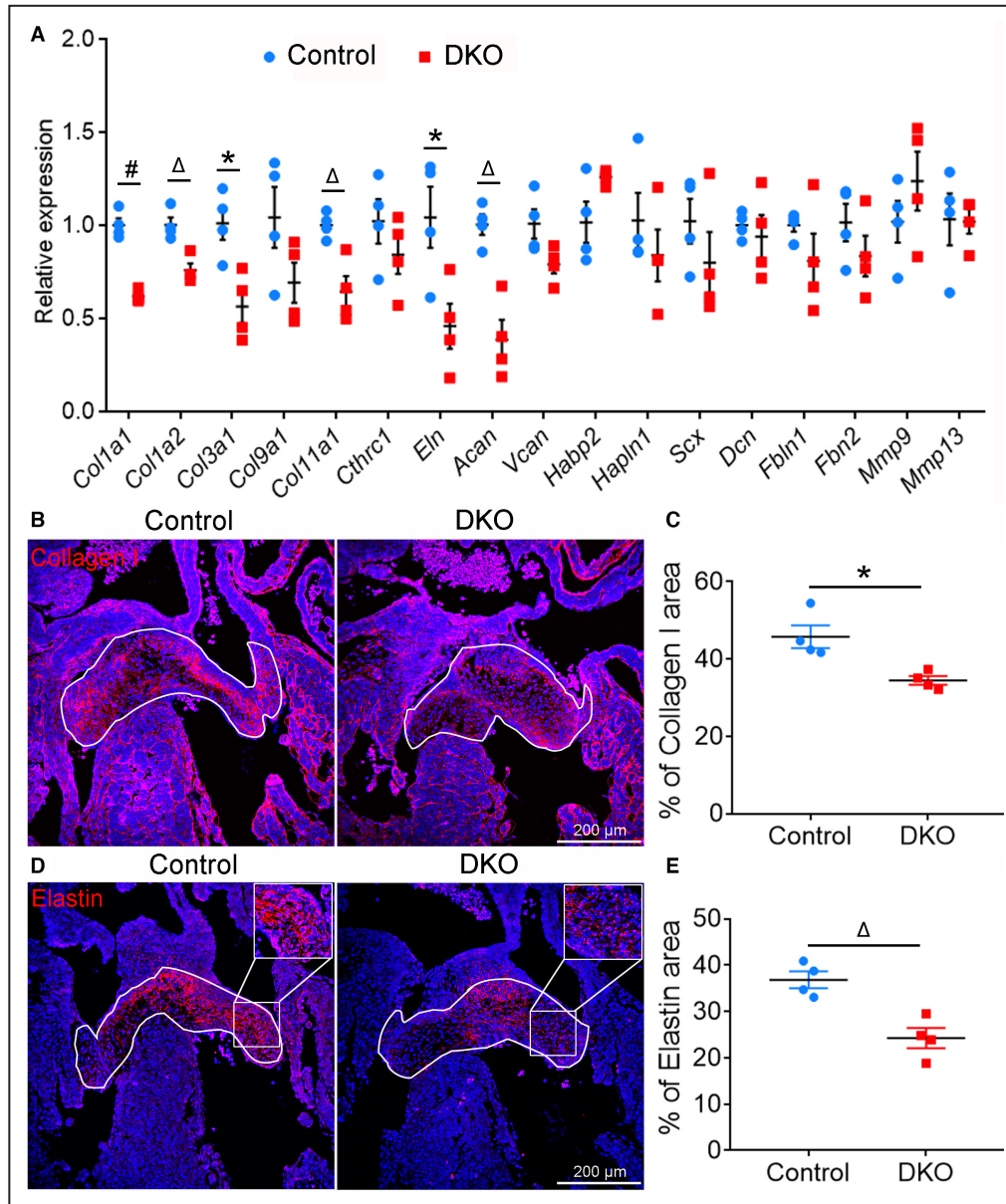
Figure 6.   Loss of endocardial *Crk* and *Crkl* impairs ECM synthesis and deposition.
A, RT-qPCR analysis shows downregulated expression of major ECM genes encoding collagens, elastin, and Acan in the atrioventricular valve regions of embryonic day 13.5 DKO hearts. The expression of *Tf2b* was used as internal control. n=4/group. **B** through **E**, Quantitative immunostaining shows dysregulated deposition of collagen I (**B** and **C**) and elastin (**D** and **E**) in the remodeling atrioventricular cushions or valves (outlined by solid lines) of embryonic day 13.5 DKO embryos. n=4/group. *$P<0.05$; $^{\Delta}P<0.01$; $^{\#}P<0.001$ by unpaired Student's *t* test. DKO indicates double knockout; ECM, extracellular matrix; and RT-qPCR, real-time quantitative polymerase chain reaction.

Endocardial *Crk* and *Crkl* Regulate Signaling Genes Involved in Valve Morphogenesis

Crk and *Crkl* play central roles in coordinating and mediating diverse cellular signaling at the protein level that can directly or indirectly affect cell apoptosis and ECM synthesis. Given the complexity of the protein activities regulated by *Crk* and *Crkl*, we decided to reveal how

Crk and *Crkl* regulate programmed cell death and ECM production in the remodeling of atrioventricular valves at the mRNA level by a candidate gene approach. We performed RT-qPCR analysis to reveal the mRNA expression of key genes involved in mesenchymal morphogenesis in the remodeling atrioventricular valves isolated from embryonic day 13.5 control versus DKO hearts. We found that the expression of transcription

factors (*Nf1*, *Msx1*, *Nfatc1*, *Id3*, *Twist1*)[9,32–35] and signaling molecules (*Bmp4*, *Bmpr1a*, *Bmpr2*, *Tgfbr2*, *Ctgf*, *Wnt4*),[10,36–38] all known for valve remodeling, was significantly reduced in the remodeling atrioventricular valves of the DKO hearts (Figure 7). Additionally, immunostaining revealed that the level of phospho-extracellular signal-regulated kinase 1/2, but not pSMAD1/5/9, was significantly reduced in the remodeling atrioventricular valves of DKO embryos when compared with their littermate controls (Figure S8), indicating that loss of *Crk* and *Crkl* affected extracellular signal-regulated kinase (ERK) signaling. Together, these findings suggest that *Crk* and *Crkl* may regulate the molecular signals at the transcriptional level, in addition to their known functions in modulating cell signaling activities at the protein level.

DISCUSSION

The heart valves are the gatekeeper for the unidirectional blood flow essential for heart development and functions.[3,39] Heart valve development is a complex process that requires precise cell functions in differentiation, migration, proliferation, and apoptosis, as well as the organized ECM deposition that provides the proper scaffold and the mechanic signaling; together, they sculpture the working heart valves.[13] These functions are tightly controlled by multiple interactive signaling pathways; genetic mutations affecting individual pathways can cause congenital heart valve disease with common structural defects, leading to significant clinical consequences. In the present study, we aimed to better understand the developmental pathogenesis
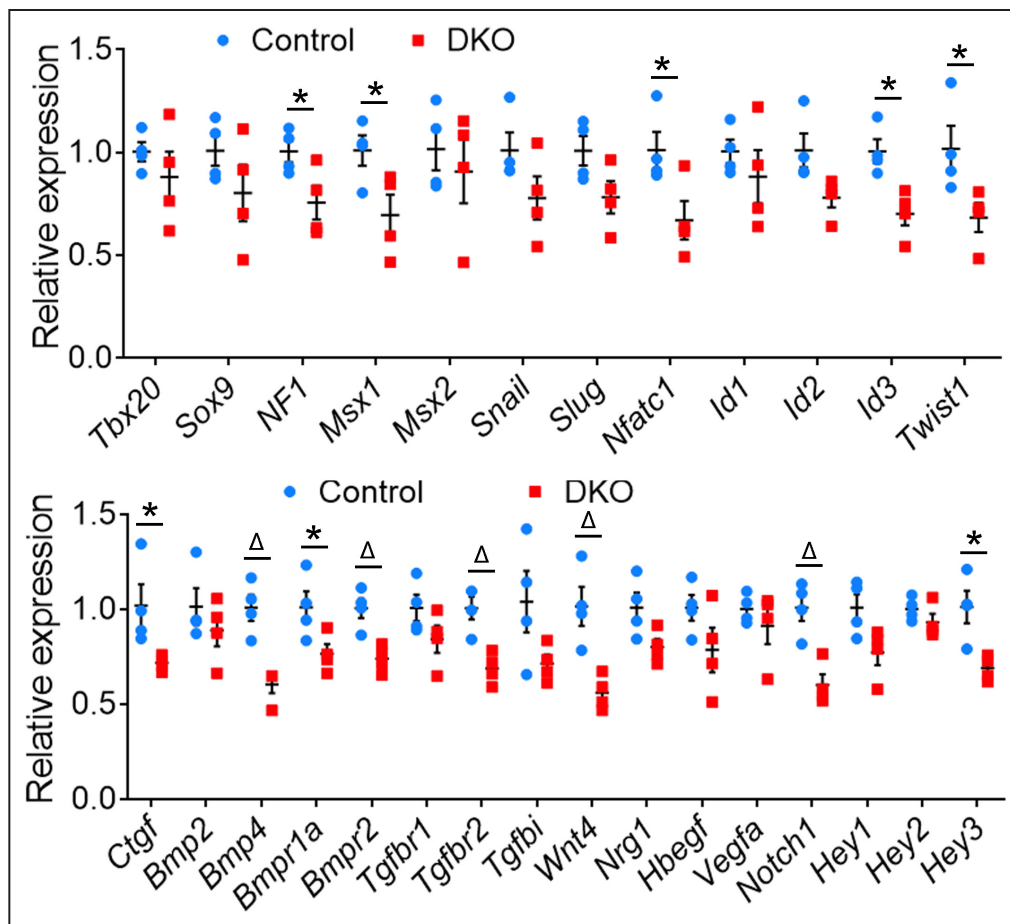

Figure 7. Characterization of molecular defects in the remodeling atrioventricular endocardial cushions and valves.
RT-qPCR analysis of the expression of genes involved in the mesenchymal tissue morphogenesis (ie, the valve remodeling) using the AVC endocardial cushions from embryonic day 13.5 control and DKO hearts. Note that there are downregulated transcription factors (*Nf1*, *Msx1*, *Nfatc1*, *Id3*, and *Twist1*) and signaling molecules (*Ctgf*, *Bmp4*, *Bmpr2*, *Tgfbr2*, *Wnt4*, *Notch1*, and *Hey3*) in the remodeling atrioventricular endocardial cushions or valves of embryonic day 13.5 DKO hearts. The expression of *Tf2b* was used as internal control. n=4/group. *P<0.05; ^ΔP<0.01 by unpaired Student's *t* test. AVC indicates atrioventricular canal; DKO, double knockout; and RT-qPCR, real-time quantitative polymerase chain reaction.

of congenital heart valve disease by studying the endocardial specific functions of 2 key signaling and human disease genes, *Crk* and *Crkl*, in the mouse model. We found that the loss of *Crk* and *Crkl* in the endocardial lineage causes anomalous atrioventricular valves and defective atrioventricular septum due to abnormal remodeling of the AVC endocardial cushions. We characterized the underlying cellular defects as the reduced developmental programmed cell death as well as altered ECM production and alignment. We further showed that *Crk* and *Crkl* regulate the mRNA level of several key genes, including transcription factors and signaling molecules involved in the post-EndMT valve remodeling (Figure 8). Together, these findings inform a previously unknown role for *Crk* and *Crkl* in the endocardial lineage for heart valve development.

Crk and *Crkl* are expressed ubiquitously in the developing mouse heart, and germline inactivation studies have shown that loss of either *Crk* or *Crkl* causes cardiovascular defects in mice.[25,28] In our study, we examined their specific tissue functions in the endocardial lineage during mouse heart development by double knockouts, as individual endocardial gene inactivation did not result in any significant heart valve defect. We found that the deletion of all 4 alleles of both genes is embryonic lethal around embryonic day 15.5 and embryonic day 16.5, suggesting that *Crk* and *Crkl* have shared functions and work redundantly in the endocardial lineage during heart development. Overlapping functions of *Crk* and *Crkl* are found in many biological systems, including neuronal and T-cell migration, neuromuscular synapse formation, podocyte morphogenesis, natural killer cell expansion and differentiation, lens fiber cell elongation, and postnatal lens capsule development.[29,40] In the developing mouse heart, *Crk* and *Crkl* have shared functions in the cardiac neural crest cells for OFT septation by regulating vascular smooth muscle differentiation and apoptosis.[30]

Here, we show that loss of *Crk* and *Crkl* in the endocardial lineage affects remodeling of AVC endocardial cushion, leading to immature atrioventricular valves with defective atrioventricular septa. Surprisingly, we did not observe morphological changes at the forming AVC endocardial cushions at embryonic day 11.5, indicating that EMT was not affected by the double deletion; however, we could not rule out a possibility of incomplete deletion and residual protein functions that might be sufficient in supporting EMT and early endocardial cushion development. Also unexpectedly, the double deletion does not affect the remodeling of OFT endocardial cushions and the formation of the semilunar valves, although the cardiac OFT defects including double-outlet right ventricular, overriding aorta, and tetralogy of Fallot are common in the *Crkl* germline null mice.[25,26,41] This difference may reflect the fact that the endocardial cell is the major progenitor cell source

for the endocardial cushion mesenchyme of the AVC and the atrioventricular valves,[11] whereas the OFT endocardial cushions and the semilunar valves are made of 3 progenitor populations in the endocardium,[10] the cardiac neural crest,[9,42–44] and the secondary heart field.[45–47] Thus, the loss of *Crk* and *Crkl* cells and functions in the endocardial lineage at OFT may be compensated by other cell lineages. Future studies are needed to attest this possibility. Nonetheless, our findings support a redundant role for *Crk* and *Crkl* in the endocardial lineage for the atrioventricular valve formation, whereas their functions in the cardiac neural crest and secondary heart field are critical for the proper alignment and separation of OFT during heart development.

One significant observation made in this study is that programmed cell death in the remodeling AVC endocardial cushions is tightly and developmentally regulated, with the peak of apoptosis occurring around embryonic day 12.5 and embryonic day 13.5 when the endocardial cushions (ie, the valve primordia) are being sculptured into the elongated valve leaflets. The loss-of-function studies indicates that *Crk* and *Crkl* are required for this developmentally regulated apoptosis in the remodeling AVC endocardial cushions. Interestingly, *Crk* and *Crkl* are also required for the cytoskeletal remodeling following acute podocyte injury in mice, and *Crk* null mouse embryonic fibroblasts are strongly resistant to endoplasmic reticulum stress–induced apoptosis, suggesting that CRK can function as a proapoptotic protein under certain pathological conditions.[48,49]

Another important finding in this study is that ECM synthesis and deposition are also temporally regulated in the remodeling AVC endocardial cushions. This is exemplified by the markedly upregulated expression of *Col1a1* and *Eln*, which are 2 major ECM proteins in the AVC endocardial cushions at embryonic day 12.5 and embryonic day 13.5, and high expression is continued to embryonic day 16.5 when the cushions are shaped into the valve leaflets. Notably, *Crk* and *Crkl* are also required for maintaining the high expression of *Col1a1* and *Eln*, as well as the proper alignment of collagen and elastin fibers that is critical for the heart valve remodeling and functions; their dysregulated deposition and alignment are associated with congenital and adult heart valve disease.[50,51] Whether apoptosis and ECM organization are functionally interacted or connected is not clear in our study; however, we show that both morphological events are dependent on the expression of *Crk* and *Crkl* in the endocardial lineage, and they are dysregulated in the remodeling AVC endocardial cushions of the double null hearts.

Crk and *Crkl* are major adaptor proteins involved in multiple cell signals by protein–protein interactions.[18] For instance, *Crk* proteins mediate the vascular endothelial growth factor signaling through the ERK, AKT, and JNK pathways to regulate proliferation, migration,
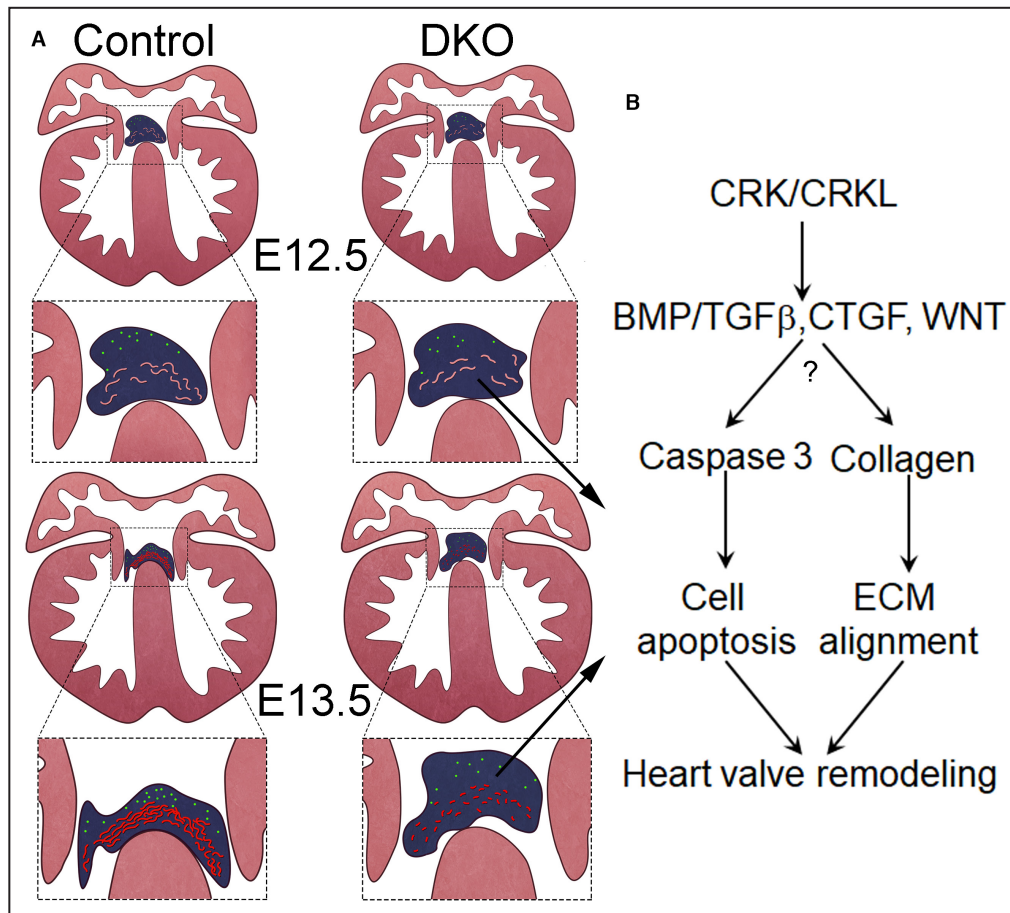
Figure 8. Schematic shows the essential roles of *Crk/Crkl* in the remodeling of atrioventricular endocardial cushions and valves.

A, Transformation of endocardial cushions into valve leaflet starts between embryonic day 12.5 and embryonic day 13.5. This process is impeded by loss of *Crk/Crkl* (DKO) in endocardial lineage. Spatiotemporally regulated apoptosis (green dots) is required for normal atrioventricular cushion remodeling at AVC. Loss of *Crk* and *Crkl* leads to markedly reduced apoptosis. Additionally, major ECM proteins, collagen and elastin (red lines), are significantly upregulated at atrioventricular cushion between embryonic day 12.5 and embryonic day 13.5 to provide the scaffold supporting valve leaflet elongation. Loss of *Crk/Crkl* results in decreased expression of both proteins and misalignment of fibrous networks. **B**, Mechanistically, our results suggest that loss of *Crk/Crkl* downregulates the expression of genes involved in the BMP/TGF-β, CTGF, and WNT signaling pathways, which together may lead to the valve morphogenic defects. AVC indicates atrioventricular canal; BMP, bone morphogenetic protein; CTGF, connective tissue growth factor; DKO, double knockout; ECM, extracellular matrix; and TGF-β, transforming growth factor-β.

survival of endothelial cells,[52] and crosstalk with transforming growth factor-β pathway in tumor cells,[53,54] whereas *Crkl* is required for fibroblast growth factor 8–induced ERK activation during OFT development.[26] In our study, we found by immunostaining that loss of *Crk* and *Crkl* resulted in reduced ERK signaling in the developing heart valves, while it had no effect on transforming growth factor-β signaling. These results suggest that reduced ERK signaling may contribute to the atrioventricular valve phenotype.

We did not attempt to dissect out the cell signaling changes at the protein or signaling level, as the combined deletion of *Crk* and *Crkl* affects the expression of genes involved in bone morphogenetic protein (BMP)/transforming growth factor-β, WNT, and connective tissue growth factor pathways, and all are critical for the valve remodeling and likely interact each other. Instead, we examined the mRNA expression of 47 candidate genes that are involved in cell signaling during tissue morphogenesis as the readout for the *Crk* and *Crkl* dependent coregulations during the valve remodeling. We found downregulation of transcription factors (*Nf1*, *Msx1*, *Nfatc1*, *Id3*, *Twist 1*) and signaling molecules (*Ctgf*, *Hey3*, *Bmp4*, *Bmpr1a*, *Bmpr2*, *Tgfbr2*, *Tgfbi*, *Wnt4*) in the remodeling AVC endocardial cushions resulting from the endocardial deletion of *Crk* and *Crkl*.

We predict that the sum of these changes may cause the signaling collapse, leading to dysregulated apoptosis and ECM synthesis, which in turn contribute to the malformation of the atrioventricular valves. Future studies are needed to identify the major signaling pathway(s) regulated by *Crk* and *Crkl* during atrioventricular valve development.

In summary, our study suggests a critical role for *Crk* and *Crkl* in the endocardial lineage for heart valve development by regulating program cell death and organized ECM synthesis and the underlying morphogenic signaling.

ARTICLE INFORMATION

Affiliations

Department of Genetics, Albert Einstein College of Medicine, Bronx, NY (B.W., B.W., S.B., L.S., P.L., B.E.M., Y.W., B.Z.); Children's Mercy Research Institute, Children's Mercy Kansas City and Department of Pediatrics, University of Missouri-Kansas City School of Medicine, Kansas City, MO (T.P.); and Cardiovascular Research Center, School of Basic Medical Sciences, Xi'an Jiaotong University Health Science Center, Xi'an, China (Y.W.).

Sources of Funding

Disclosures

None.

Supplemental Material

Tables S1–S2
Figures S1–S8

REFERENCES

1. van der Linde D, Konings EE, Slager MA, Witsenburg M, Helbing WA, Takkenberg JJ, Roos-Hesselink JW. Birth prevalence of congenital heart disease worldwide: a systematic review and meta-analysis. *J Am Coll Cardiol*. 2011;58:2241–2247. doi: 10.1016/j.jacc.2011.08.025

2. Hoffman JI, Kaplan S. The incidence of congenital heart disease. *J Am Coll Cardiol*. 2002;39:1890–1900. doi: 10.1016/s0735-1097(02)01886-7

3. Armstrong EJ, Bischoff J. Heart valve development: endothelial cell signaling and differentiation. *Circ Res*. 2004;95:459–470. doi: 10.1161/01.RES.0000141146.95728.da

4. van der Bom T, Zomer AC, Zwinderman AH, Meijboom FJ, Bouma BJ, Mulder BJ. The changing epidemiology of congenital heart disease. *Nat Rev Cardiol*. 2011;8:50–60. doi: 10.1038/nrcardio.2010.166

5. Bruneau BG. The developmental genetics of congenital heart disease. *Nature*. 2008;451:943–948. doi: 10.1038/nature06801

6. Bouma BJ, Mulder BJ. Changing landscape of congenital heart disease. *Circ Res*. 2017;120:908–922. doi: 10.1161/CIRCRESAHA.116.309302

7. Yutzey KE, Demer LL, Body SC, Huggins GS, Towler DA, Giachelli CM, Hofmann-Bowman MA, Mortlock DP, Rogers MB, Sadeghi MM, et al. Calcific aortic valve disease: a consensus summary from the Alliance of investigators on calcific aortic valve disease. *Arterioscler Thromb Vasc Biol*. 2014;34:2387–2393. doi: 10.1161/ATVBAHA.114.302523

8. Combs MD, Yutzey KE. Heart valve development: regulatory networks in development and disease. *Circ Res*. 2009;105:408–421. doi: 10.1161/CIRCRESAHA.109.201566

9. Wu B, Wang Y, Lui W, Langworthy M, Tompkins KL, Hatzopoulos AK, Baldwin HS, Zhou B. Nfatc1 coordinates valve endocardial cell lineage development required for heart valve formation. *Circ Res*. 2011;109:183–192. doi: 10.1161/CIRCRESAHA.111.245035

10. Wang Y, Wu B, Chamberlain AA, Lui W, Koirala P, Susztak K, Klein D, Taylor V, Zhou B. Endocardial to myocardial notch-wnt-bmp axis regulates early heart valve development. *PLoS One*. 2013;8:e60244. doi: 10.1371/journal.pone.0060244

11. de Lange FJ, Moorman AF, Anderson RH, Manner J, Soufan AT, de Gier-de VC, Schneider MD, Webb S, van den Hoff MJ, Christoffels VM. Lineage and morphogenetic analysis of the cardiac valves. *Circ Res*. 2004;95:645–654. doi: 10.1161/01.RES.0000141429.13560.cb

12. Wang Y, Wu B, Farrar E, Lui W, Lu P, Zhang D, Alfieri CM, Mao K, Chu M, Yang D, et al. Notch-Tnf signalling is required for development and homeostasis of arterial valves. *Eur Heart J*. 2017;38:675–686. doi: 10.1093/eurheartj/ehv520

13. Lin CJ, Lin CY, Chen CH, Zhou B, Chang CP. Partitioning the heart: mechanisms of cardiac septation and valve development. *Development*. 2012;139:3277–3299. doi: 10.1242/dev.063495

14. Luxan G, D'Amato G, MacGrogan D, de la Pompa JL. Endocardial notch signaling in cardiac development and disease. *Circ Res*. 2016;118:e1–e18. doi: 10.1161/CIRCRESAHA.115.305350

15. Matsuda M, Tanaka S, Nagata S, Kojima A, Kurata T, Shibuya M. Two species of human CRK cDNA encode proteins with distinct biological activities. *Mol Cell Biol*. 1992;12:3482–3489. doi: 10.1128/mcb.12.8.3482

16. ten Hoeve J, Morris C, Heisterkamp N, Groffen J. Isolation and chromosomal localization of CRKL, a human crk-like gene. *Oncogene*. 1993;8:2469–2474.

17. Prosser S, Sorokina E, Pratt P, Sorokin A. CrkIII: a novel and biologically distinct member of the Crk family of adaptor proteins. *Oncogene*. 2003;22:4799–4806. doi: 10.1038/sj.onc.1206714

18. Birge RB, Kalodimos C, Inagaki F, Tanaka S. Crk and CrkL adaptor proteins: networks for physiological and pathological signaling. *Cell Commun Signal*. 2009;7:13. doi: 10.1186/1478-811X-7-13

19. Imamoto A, Ki S, Li L, Iwamoto K, Maruthamuthu V, Devany J, Lu O, Kanazawa T, Zhang S, Yamada T, et al. Essential role of the Crk family-dosage in DiGeorge-like anomaly and metabolic homeostasis. *Life Sci Alliance*. 2020;3:3. doi: 10.26508/lsa.201900635

20. Miller JQ. Lissencephaly in 2 siblings. *Neurology*. 1963;13:841–850. doi: 10.1212/wnl.13.10.841

21. Pilz DT, Quarrell OW. Syndromes with lissencephaly. *J Med Genet*. 1996;33:319–323. doi: 10.1136/jmg.33.4.319

22. Nagamani SC, Zhang F, Shchelochkov OA, Bi W, Ou Z, Scaglia F, Probst FJ, Shinawi M, Eng C, Hunter JV, et al. Microdeletions including YWHAE in the Miller-Dieker syndrome region on chromosome 17p13.3 result in facial dysmorphisms, growth restriction, and cognitive impairment. *J Med Genet*. 2009;46:825–833. doi: 10.1136/jmg.2009.067637

23. Racedo SE, McDonald-McGinn DM, Chung JH, Goldmuntz E, Zackai E, Emanuel BS, Zhou B, Funke B, Morrow BE. Mouse and human CRKL is dosage sensitive for cardiac outflow tract formation. *Am J Hum Genet*. 2015;96:235–244. doi: 10.1016/j.ajhg.2014.12.025

24. Barros Fontes MI, Dos Santos AP, Rossi Torres F, Lopes-Cendes I, Cendes F, Appenzeller S, Kawasaki de Araujo T, Lopes Monlleo I, Gil-da-Silva-Lopes VL. 17p13.3 microdeletion: insights on genotype-phenotype correlation. *Mol Syndromol*. 2017;8:36–41. doi: 10.1159/000452753

25. Guris DL, Fantes J, Tara D, Druker BJ, Imamoto A. Mice lacking the homologue of the human 22q11.2 gene CRKL phenocopy neurocristopathies of DiGeorge syndrome. *Nat Genet*. 2001;27:293–298. doi: 10.1038/85855

26. Moon AM, Guris DL, Seo JH, Li L, Hammond J, Talbot A, Imamoto A. Crkl deficiency disrupts Fgf8 signaling in a mouse model of 22q11 deletion syndromes. *Dev Cell*. 2006;10:71–80. doi: 10.1016/j.devcel.2005.12.003

27. Guris DL, Duester G, Papaioannou VE, Imamoto A. Dose-dependent interaction of Tbx1 and Crkl and locally aberrant RA signaling in a model of del22q11 syndrome. *Dev Cell*. 2006;10:81–92. doi: 10.1016/j.devcel.2005.12.002

28. Park TJ, Boyd K, Curran T. Cardiovascular and craniofacial defects in Crk-null mice. *Mol Cell Biol*. 2006;26:6272–6282. doi: 10.1128/MCB.00472-06

29. Park TJ, Curran T. Crk and Crk-like play essential overlapping roles downstream of disabled-1 in the reelin pathway. *J Neurosci*. 2008;28:13551–13562. doi: 10.1523/JNEUROSCI.4323-08.2008

30. Shi L, Racedo SE, Diacou A, Park T, Zhou B, Morrow BE. Crk and Crkl have shared functions in neural crest cells for cardiac outflow tract

septation and vascular smooth muscle differentiation. *Hum Mol Genet*. 2022;31:1197–1215. doi: 10.1093/hmg/ddab313

31. Wu B, Zhang Z, Lui W, Chen X, Wang Y, Chamberlain AA, Moreno-Rodriguez RA, Markwald RR, O'Rourke BP, Sharp DJ, et al. Endocardial cells form the coronary arteries by angiogenesis through myocardial-endocardial VEGF signaling. *Cell*. 2012;151:1083–1096. doi: 10.1016/j.cell.2012.10.023

32. Chen YH, Ishii M, Sucov HM, Maxson RE Jr. Msx1 and Msx2 are required for endothelial-mesenchymal transformation of the atrioventricular cushions and patterning of the atrioventricular myocardium. *BMC Dev Biol*. 2008;8:75. doi: 10.1186/1471-213X-8-75

33. Chakraborty S, Cheek J, Sakthivel B, Aronow BJ, Yutzey KE. Shared gene expression profiles in developing heart valves and osteoblast progenitor cells. *Physiol Genomics*. 2008;35:75–85. doi: 10.1152/physiolgenomics.90212.2008

34. Brannan CI, Perkins AS, Vogel KS, Ratner N, Nordlund ML, Reid SW, Buchberg AM, Jenkins NA, Parada LF, Copeland NG. Targeted disruption of the neurofibromatosis type-1 gene leads to developmental abnormalities in heart and various neural crest-derived tissues. *Genes Dev*. 1994;8:1019–1029. doi: 10.1101/gad.8.9.1019

35. Hu W, Xin Y, Hu J, Sun Y, Zhao Y. Inhibitor of DNA binding in heart development and cardiovascular diseases. *Cell Commun Signal*. 2019;17:51. doi: 10.1186/s12964-019-0365-z

36. McCulley DJ, Kang JO, Martin JF, Black BL. BMP4 is required in the anterior heart field and its derivatives for endocardial cushion remodeling, outflow tract septation, and semilunar valve development. *Dev Dyn*. 2008;237:3200–3209. doi: 10.1002/dvdy.21743

37. Ma L, Lu MF, Schwartz RJ, Martin JF. Bmp2 is essential for cardiac cushion epithelial-mesenchymal transition and myocardial patterning. *Development*. 2005;132:5601–5611. doi: 10.1242/dev.02156

38. Robson A, Allinson KR, Anderson RH, Henderson DJ, Arthur HM. The TGFbeta type II receptor plays a critical role in the endothelial cells during cardiac development. *Dev Dyn*. 2010;239:2435–2442. doi: 10.1002/dvdy.22376

39. Hinton RB, Yutzey KE. Heart valve structure and function in development and disease. *Annu Rev Physiol*. 2011;73:29–46. doi: 10.1146/annurev-physiol-012110-142145

40. Park T. Crk and CrkL as therapeutic targets for cancer treatment. *Cells*. 2021;10. doi: 10.3390/cells10040739

41. Breckpot J, Thienpont B, Bauters M, Tranchevent LC, Gewillig M, Allegaert K, Vermeesch JR, Moreau Y, Devriendt K. Congenital heart defects in a novel recurrent 22q11.2 deletion harboring the genes CRKL and MAPK1. *Am J Med Genet A*. 2012;158A:574–580. doi: 10.1002/ajmg.a.35217

42. Brown CB, Feiner L, Lu MM, Li J, Ma X, Webber AL, Jia L, Raper JA, Epstein JA. PlexinA2 and semaphorin signaling during cardiac neural crest development. *Development*. 2001;128:3071–3080. doi: 10.1242/dev.128.16.3071

43. Feiner L, Webber AL, Brown CB, Lu MM, Jia L, Feinstein P, Mombaerts P, Epstein JA, Raper JA. Targeted disruption of semaphorin 3C leads to

44. Toyofuku T, Yoshida J, Sugimoto T, Yamamoto M, Makino N, Takamatsu H, Takegahara N, Suto F, Hori M, Fujisawa H, et al. Repulsive and attractive semaphorins cooperate to direct the navigation of cardiac neural crest cells. *Dev Biol*. 2008;321:251–262. doi: 10.1016/j.ydbio.2008.06.028

45. Cai CL, Liang X, Shi Y, Chu PH, Pfaff SL, Chen J, Evans S. Isl1 identifies a cardiac progenitor population that proliferates prior to differentiation and contributes a majority of cells to the heart. *Dev Cell*. 2003;5:877–889. doi: 10.1016/s1534-5807(03)00363-0

46. Verzi MP, McCulley DJ, De Val S, Dodou E, Black BL. The right ventricle, outflow tract, and ventricular septum comprise a restricted expression domain within the secondary/anterior heart field. *Dev Biol*. 2005;287:134–145. doi: 10.1016/j.ydbio.2005.08.041

47. Snarr BS, Wirrig EE, Phelps AL, Trusk TC, Wessels A. A spatiotemporal evaluation of the contribution of the dorsal mesenchymal protrusion to cardiac development. *Dev Dyn*. 2007;236:1287–1294. doi: 10.1002/dvdy.21074

48. George B, Fan Q, Dlugos CP, Soofi AA, Zhang J, Verma R, Park TJ, Wong H, Curran T, Nihalani D, et al. Crk1/2 and CrkL form a heterooligomer and functionally complement each other during podocyte morphogenesis. *Kidney Int*. 2014;85:1382–1394. doi: 10.1038/ki.2013.556

49. Austgen K, Johnson ET, Park TJ, Curran T, Oakes SA. The adaptor protein CRK is a pro-apoptotic transducer of endoplasmic reticulum stress. *Nat Cell Biol*. 2011;14:87–92. doi: 10.1038/ncb2395

50. Hinton RB Jr, Lincoln J, Deutsch GH, Osinska H, Manning PB, Benson DW, Yutzey KE. Extracellular matrix remodeling and organization in developing and diseased aortic valves. *Circ Res*. 2006;98:1431–1438. doi: 10.1161/01.RES.0000224114.65109.4e

51. Gomez-Stallons MV, Tretter JT, Hassel K, Gonzalez-Ramos O, Amofa D, Ollberding NJ, Mazur W, Choo JK, Smith JM, Kereiakes DJ, et al. Calcification and extracellular matrix dysregulation in human postmortem and surgical aortic valves. *Heart*. 2019;105:1616–1621. doi: 10.1136/heartjnl-2019-314879

52. Salameh A, Galvagni F, Bardelli M, Bussolino F, Oliviero S. Direct recruitment of CRK and GRB2 to VEGFR-3 induces proliferation, migration, and survival of endothelial cells through the activation of ERK, AKT, and JNK pathways. *Blood*. 2005;106:3423–3431. doi: 10.1182/blood-2005-04-1388

53. Cheng S, Guo J, Yang Q, Han L. Crk-like adapter protein is required for TGF-beta-induced AKT and ERK-signaling pathway in epithelial ovarian carcinomas. *Tumour Biol*. 2015;36:915–919. doi: 10.1007/s13277-014-2724-0

54. Elmansuri AZ, Tanino MA, Mahabir R, Wang L, Kimura T, Nishihara H, Kinoshita I, Dosaka-Akita H, Tsuda M, Tanaka S. Novel signaling collaboration between TGF-beta and adaptor protein Crk facilitates EMT in human lung cancer. *Oncotarget*. 2016;7:27094–27107. doi: 10.18632/oncotarget.8314

Supplemental Material

Table S1. A list of antibodies used in this study.

Antibodies	Manufacture	Cat #	Dilution (IF)
Caspase3	CST	#9664	1:100
Collagen I	Abcam	ab34710	1:100
CRK	BD	610036	1:100
Elastin	Abcam	ab21600	1:100
HABP2	Abcam	ab181837	1:100
pERK1/2	CST	#9101	1:100
pH3	CST	#9701	1:100
pSMAD1/5/9	CST	#13820	1:100
SLUG	CST	#9585	1:100
SOX9	R&D system	AF3075	1:100
TWIST1	Santa Cruz	Sc-8417	1:100
Versican	Abcam	ab177480	1:100

Table S2. A list of primers used in this study.

Gene	NCBI reference number	Primer sequence (Related to Fig. 3E)
Fasl	NM_001205243	5'-GCAGAGGCACAGAGAAAGAA-3' 5'-CACCCTGGAAGTGAGTGTAAAG-3'
Fas	NM_007987.2	5'-CTTGCTGGCTCACAGTTAAGA-3' 5'-GGGCCTCCTTGATATAATCCTTC-3'
Tnf	NM_013693	5'-CTACCTTGTTGCCTCCTCTTT-3' 5'-GAGCAGAGGTTCAGTGATGTAG-3'
Tnfsf10	NM_009425	5'-CAGCCCTAAAGTACCCAGTAATC-3' 5'-CACATCTGTCCTGAGGTTTCTAC-3'
Tnfsf12	NM_011614	5'-AGTCCTGTCCTCTCCTCAAA-3' 5'-TGGTGGGATGGGATGTTAAAG-3'
Tnfsf15	NM_177371	5'-GAGGCTCACAGTAGCAAGTAAA-3' 5'-CAGCCTGTATACCCTCTGAAAC-3'
Tnfr1	NM_011609	5'-GCTAGGTCTTTGCCTTCTATCC-3' 5'-CTTTCCAGCCTTCTCCTCTTT-3'
Tnfr2	NM_011610	5'-GAGTTGGATCCCTGACCATAAG-3' 5'-GTGAGTGTGTGTGCAAGAATG-3'
Casp3	NM_009810	5'-CAGTGGACTCTGGGATCTATCT-3' 5'-TGACATTCCAGTGCTCTTATGG-3'
Casp8	NM_001080126	5'-GACAGGAGGAACAAGGGAAAG-3' 5'-TGTGGAGAGCACACATCATTAG-3'
Bad	NM_007522.3	5'-AGGATGAGCGATGAGTTTGAG-3' 5'-TCCCACCAGGACTGGATAA-3'
Bax	NM_007527.4	5'-GTGGTTGCCCTCTTCTACTTT-3' 5'-CAGCCCATGATGGTTCTGAT-3'
Bid	NM_007544.4	5'-GAACAGCTGTCTCCCTATTTCC-3' 5'-CCGGCGTAAACTCTTCAGATAC-3'
Bim	NM_001284410.3	5'-TCCAGTACATTGGGATGATGTTAG-3' 5'-CTCTCCAGAGCTTACGGATAGA-3'
Bcl2	NM_009741.5	5'-GAGCAGGTGCCTACAAGAAA-3' 5'-CTTTGTCCTCTGACTGGGTATG-3'
Bclw	NM_001417491.1	5'-GTGGGTAGAAGCTTTGGTAGTT-3' 5'-GCTGGATAGAGAGACCCTAGAA-3'

| Gene	NCBI reference number	Primer sequence (Related to Fig. 4A)
Col1a1	NM_007742	5'-TTCTCCTGGCAAAGACGGACTCAA-3' 5'-AGGAAGCTGAAGTCATAACCGCCA-3'
Col1a2	NM_007743.3	5'-CCAGAGTGGAACAGCGATTAC-3'

Gene	NCBI reference number	Primer sequence
Col3a1	NM_009930.2	5'-GATGCAGGTTTCACCAGTAGAG-3' 5'-AGCTTTGTGCAAAGTGGAACCTGG-3'
Col9a1	NM_007740.3	5'-CAAGGTGGCTGCATCCCAATTCAT-3' 5'-GGGAGACAGAGGCATTCAAG-3'
Col11a1	NM_007729	5'-GTATTCCATCTCGGCCATCTAC-3' 5'-AGTTGGTCTGCAGTGGCAATTTCG-3'
Cthrc1	NM_026778.3	5'-AGATCCCAGATCCACCGTTTCGTT-3' 5'-CCCATCGAAGCCATCATCTATC-3'
Eln	NM_007925	5'-CAATCCCTTCACAGAGTCCTTC-3' 5'-CTACTGCTTGGTGGAGAATGT-3'
Acan	NM_007424	5'-TTCCTTGTCCTGTGGGTTTC-3' 5'-TCTGGCTTTCCAACTGTCTCCCTT-3'
Vcan	NM_001081249	5'-ACTTCTCCTGAACCACTGATGCCA -3' 5'-TCCAGGAGAAACAGTTGGGATGCT-3'
Habp2	XM_006527014	5'-AAGGAAGGAAAGGTTGGCCTCTCA-3' 5'-GAACAGAGAGGCCTTCAACTAC-3'
Hapln1	NM_013500.4	5'-GAGAGCCCAATGACTGACTTC-3' 5'-GAGGTGATTGAAGGGCTAGAAG-3'
Scx	NM_198885.3	5'-GTCCCAGTCGTGGAAAGTAAG-3' 5'-TCTGCCTCAGCAACCAGAGAAAGT-3'
Dcn	NM_001190451.2	5'-ACTCTTCAGTGGCATCCACCTTCA-3' 5'-GGTCGTCTACCTTCACAACAA-3'
Fbln1	NM_001347088.1	5'-GTAAAGACTCACAGCCGAGTAG-3' 5'-GTGCTAATGTCTATGGCTCCTAC-3'
Fbn2	NM_010181.2	5'-CAGGGCACACTCATCAATATCT-3' 5'-GAGCACAATGAGGACGACTAC-3'
Mmp9	NM_013599	5'-CAAGTCTGCAGAGGGCTAATAC-3' 5'-TGAACAAGGTGGACCATGAGGTGA-3'
Mmp13	NM_008607	5'-TAGAGACTTGCACTGCACGGTTGA -3' 5'-TGGCTTAGAGGTGACTGGCAAACT-3' 5'-TATTCACCCACATCAGGCACTCCA -3'

Gene	NCBI reference number	Primer sequence (Related to Fig. 7)
Tbx20	NM_194263	5'-CGCTTTGCTTGCTCTCTGGAACTT-3' 5'-TGCTCAGGAACCTGGACTGACAAA-3'
Sox9	NM_011448	5'-GAAAGGAAGGAAGGAAGGAAGG-3' 5'-TAAAGCTCACCAATGCTCTATGT-3'
Nf1	NM_010897	5'-ATCTGCCTGGCTCAGAATTCACCT-3' 5'-AACGCAGAATTGGTGATGATGCGG-3'
Msx1	NM_010835	5'-TCCTGGTTGTCGCTTCCTAAACCT-3' 5'-TAAATCTCTTGGCCTCTGCACCCT-3'

| Gene	Accession	Primer sequences
Msx2	NM_013601	5'-TGAGGAAACACAAGACCAACCGGA-3' 5'-ACAGGTACTGTTTCTGGCGGAACT-3'
Snail	NM_011427	5'-ACAGCTGCTTCGAGCCATAGAACT-3' 5'-TGTACCTCAAAGAAGGTGGCCTGA-3'
Slug	NM_011415	5'-ACTACAGCGAACTGGACACACACA-3' 5'-AAAGGCCACTGGGTAAAGGAGAGT-3'
Nfatc1	NM_001164109	5'-AGATGGTGCTGTCTGGCCATAACT-3' 5'-TGGTTGCGGAAAGGTGGTATCTCA-3'
Id1	NM_010495	5'-TTCTCAGGATCATGAAGGTCGCCA-3' 5'-TTTGCTCCGACAGACCAAGTACCA-3'
Id2	NM_010496	5'-TGCCCAATGTAAGCAGACTTTGCC-3' 5'-ACAGCATTCAGTAGGCTCGTGTCA-3'
Id3	NM_008321	5'-TACTCTCCAACATGAAGGCGCTGA-3' 5'-AGCAGTGGTTCATGTCGTCCAAGA-3'
Twist1	NM_011658	5'-AGTCTGAACACTCGTTTGTGTCCC-3' 5'-ATGCCTTTCCTGTCAGTGGCTGAT-3'
Ctgf	NM_010217.2	5'-ACCTGTGCCTGCCATTAC-3' 5'-GTCCCTTACTTCCTGGCTTTAC-3'
Bmp2	NM_007553	5'-TGTGGGCCCTCATAAAGAAGCAGA-3' 5'-AGCAAGCTGACAGGTCAGAGAACA-3'
Bmp4	NM_007554	5'-TGGCTCCCAAGAATCATGGACTGT-3' 5'-ACCATCAGCATTCGGTTACCAGGA-3'
Bmpr1a	NM_009758	5'-AATGCAAGGATTCACCGAAAGCCC-3' 5'-ACAGCCATGGAAATGAGCACAACC-3'
Bmpr2	NM_007561	5'-TGGCAGTGAGGTCACTCAAGGAAA-3' 5'-GCAGTTGACATTGGGTTGACCGTT -3'
Tgfbr1	NM_009370	5'-TGTCAAAGTCAGTCCGTTGGGTCT-3' 5'-ACTTTGAAAGCCACACAAGCCCTG-3'
Tgfbr2	NM_009371	5'-AGATGGCTCGCTGAACACTACCAA-3' 5'-AGAATCCTGCTGCCTCTGGTCTTT-3'
Tgfbi	NM_009369.5	5'-GCATTGCTGCCCATGATAAG-3' 5'-CTCCCTTCAGGACATCCATAAC-3'
Wnt4	NM_009523	5'-ACTGCCCAGGCCAAAGAAATTCAC-3' 5'-ATATGCTGAGCTACGTCACGCCTT-3'
Nrg1	NM_178591	5'-AAACGACCCAGGAGTATGAGCCAA-3' 5'-TTGGGTTGCTGTCCATTTCCAACC-3'
Hbegf	NM_010415	5'-TTATCCTGCTGTTCTTCGGGTGCT-3' 5'-TCAACTCCAAAGCTCCCTGCTCTT-3'
Vegfa	NM_001025250	5'-TCACCAAAGCCAGCACATAGGAGA-3' 5'-TTTCTCCGCTCTGAACAAGGCTCA-3'
Notch1	NM_008714	5'-AGTGTCAGAGGCCAGCAAGAAGAA-3'

Hey1	NM_010423	5'-TGATTGTCGTCCATCAGAGCACCA-3'
		5'-GAAACTTGAGTTCGGCGCTGTGTT-3'
		5'-AGATCCCTGCTTCTCAAAGGCACT-3'
Hey1	NM_013904	5'-AGGCTACTTTGATGCCCATGCTCT-3'
		5'-ACCTAGCCACTTCTGTCAAGCACT-3'
Hey3	NM_013905	5'-AGCATAGTCCCAATCCCACCATGT-3'
		5'-TGGTTGTGGGAAGTCAGCTCAGAA-3'

**Figure S1. Semi-quantification of CRK protein level (A) and *Crkl* mRNA level (C) in the AVC endocardial cushion.**
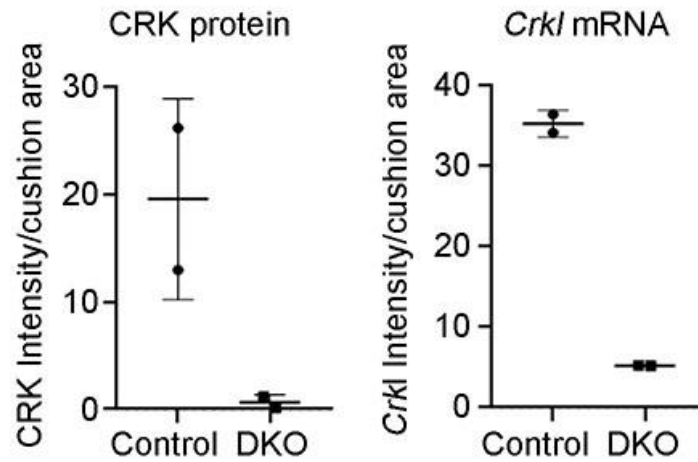
The bar charts show the semi-quantification results of the CRK protein level (showed in Figure 1A) and *Crkl* mRNA level (showed in Figure 1C) in the AVC endocardial cushion. AVC, atrioventricular canal. DKO, *Crk* and *Crkl* double knockout.

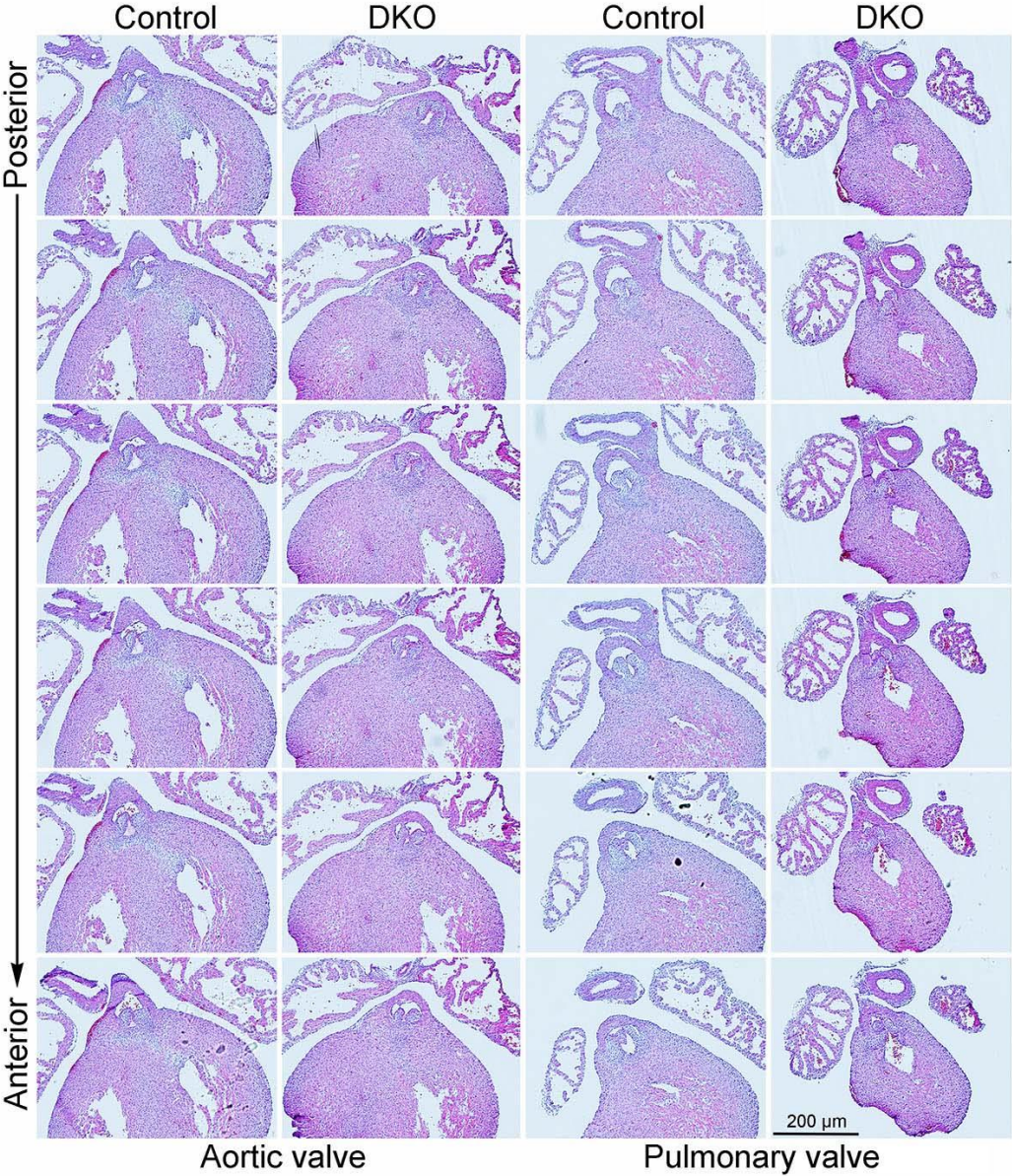**Figure S2. Loss of *Crk* and *Crkl* in the endocardial lineage does not affect endocardial cushion formation at AVC and OFT.**
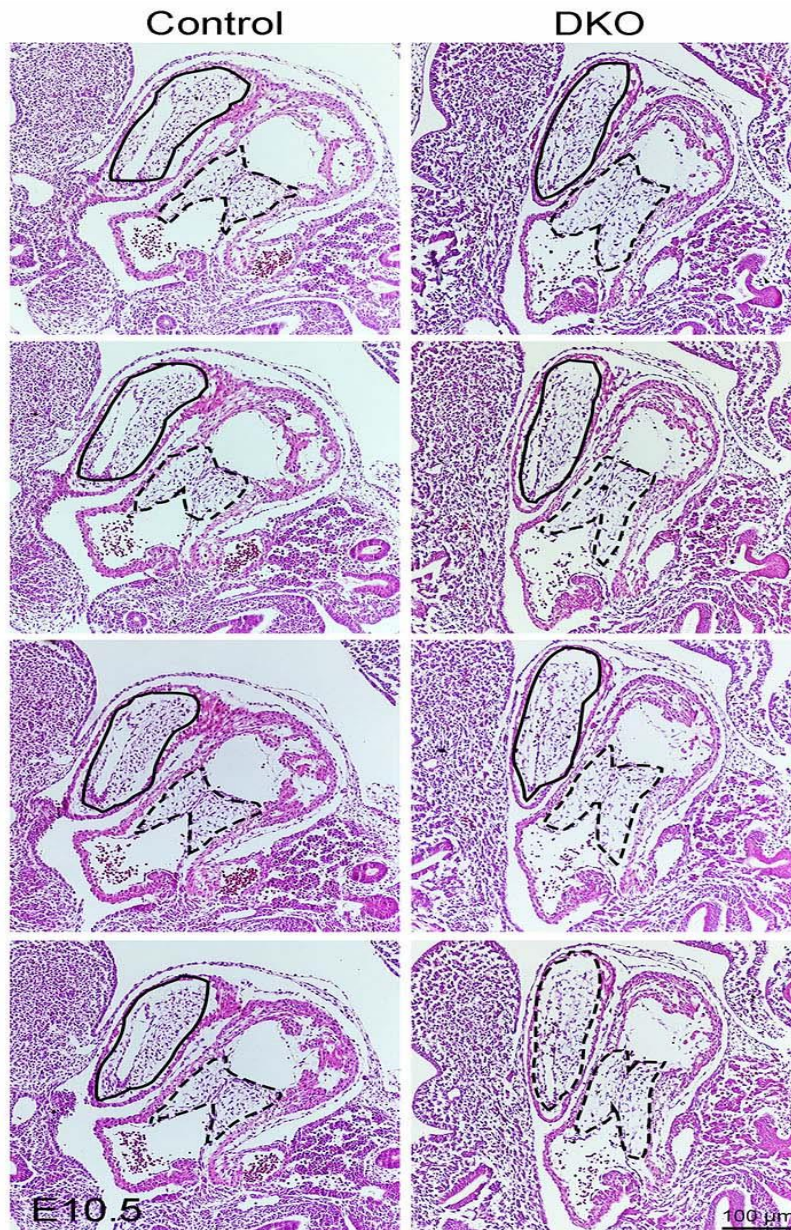
H&E stained serial sections of E10.5 control and DKO hearts across the endocardial cushion regions at AVC and OFT outlined by dashed and solid lines, respectively. AVC, atrioventricular canal. OFT, outflow tract. DKO, *Crk* and *Crkl* double knockout.

Figure S3. Loss of *Crk* and *Crkl* in the endocardial lineage does not affect the formation of OFT endocardial cushions.
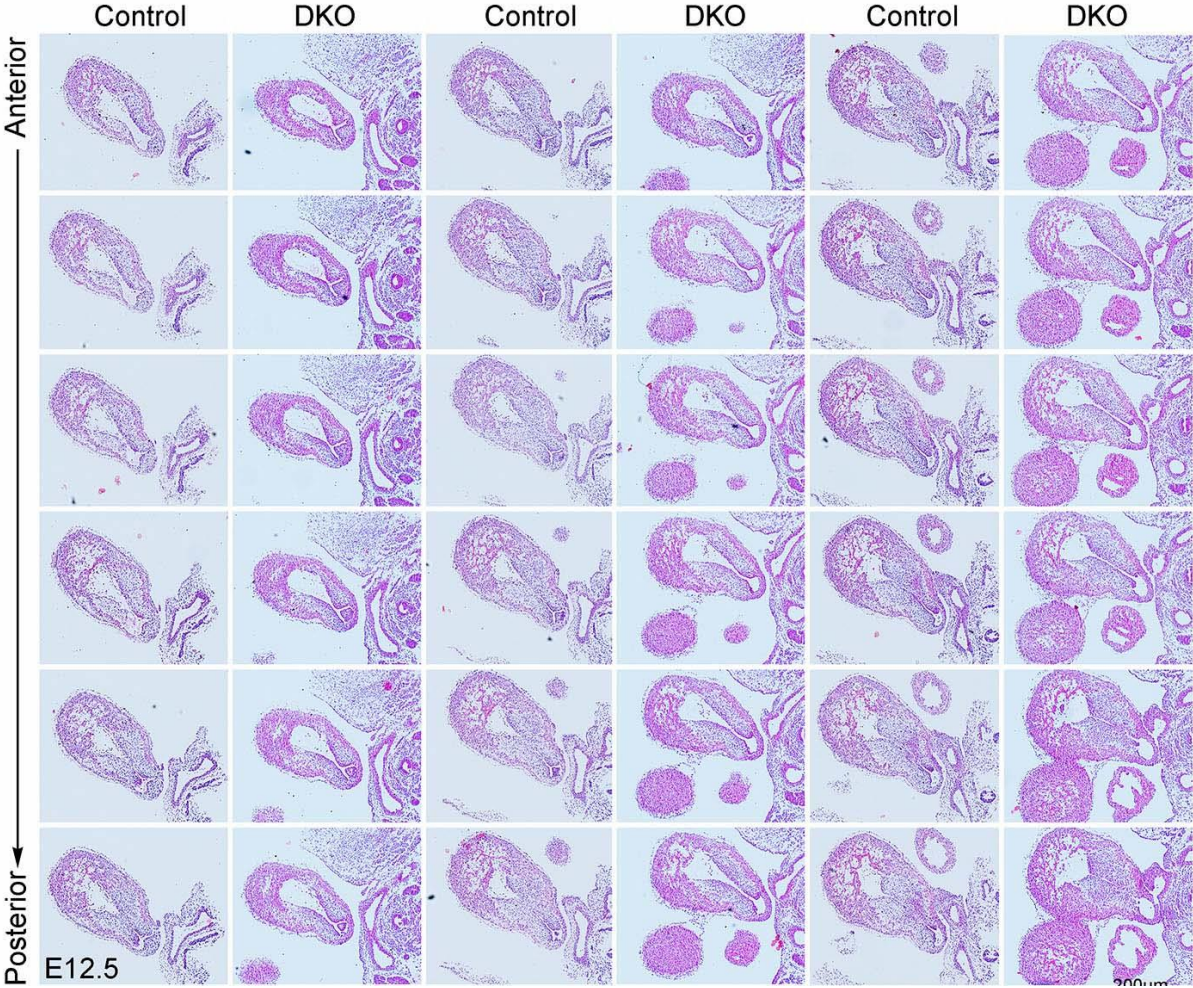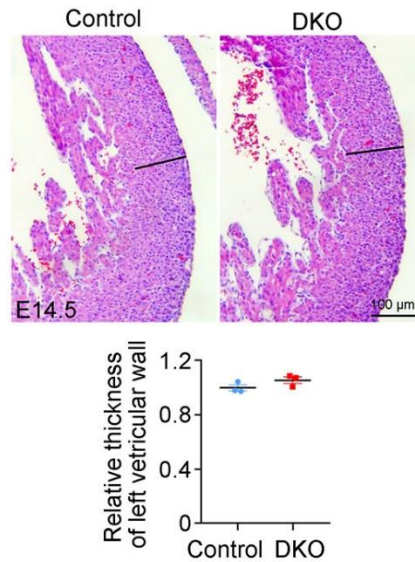

H&E stained serial sections across the OFT endocardial cushions of E12.5 control and DKO embryos show comparable morphology. OFT, outflow tract. DKO, *Crk* and *Crkl* double knockout.

Figure S4. Loss of *Crk* and *Crkl* in the endocardial lineage does not affect semilunar valve development.


H&E stained serial sections across the forming semilunar valves of E14.5 control and DKO embryos show comparable morphology. DKO, *Crk* and *Crkl* double knockout.

Figure S5. Loss of *Crk* and *Crkl* in the endocardial lineage does not affect myocardial development of E14.5 heart.


H&E stained serial sections of E14.5 hearts show morphology of left ventricular region. The bar chart shows the quantification for the thickness of ventricular free wall. n=3/group. DKO, *Crk* and *Crkl* double knockout.

Figure S6. Loss of *Crk* and *Crkl* in the endocardial lineage does not affect cell proliferation in the remodeling AVC endocardial cushions.
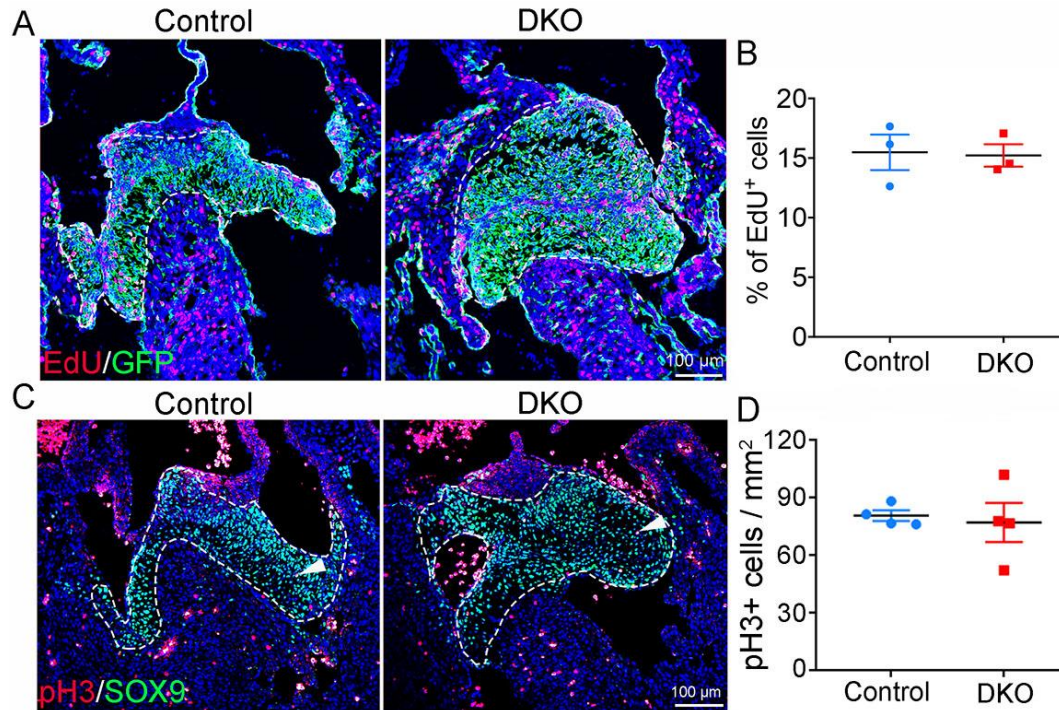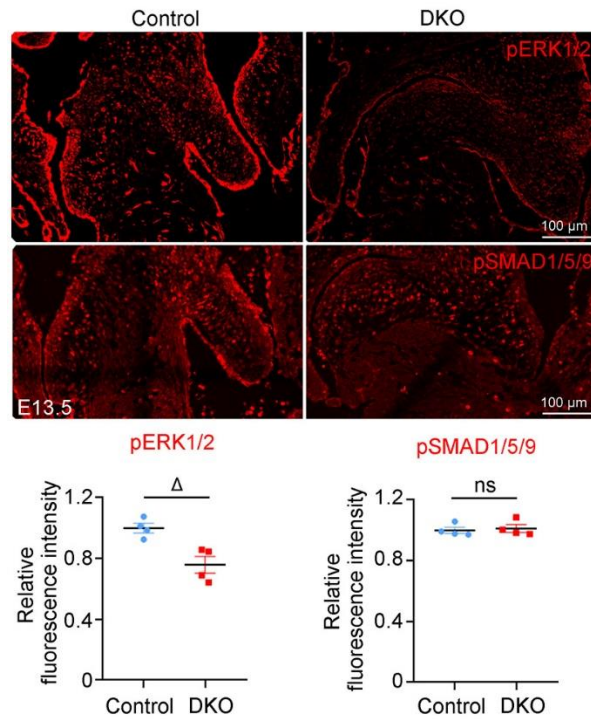

A, Representative images of EdU assays showing EdU+ (red) proliferative cells in the forming atrioventricular valves derived from endocardial cells positive for the lineage marker GFP (green) of E13.5 control and DKO embryos. **B**, Bar graph showing the quantification of the proliferative cells. n=3/group. **C**, Representative immunostaining images showing the proliferative cells expressing pH3 (red) in the remodeling atrioventricular valves expressing mesenchymal marker SOX9 (green) of E13.5 control and DKO embryos. **D**, Bar graph showing the quantification of pH3 positive cells (the ratio of pH3 positive cells among all SOX9-expressing mesenchymal cells). n=4/group. Unpaired Student's *t*-Test was used for statistical calculation. DKO, *Crk* and *Crkl* double knockout.

Figure S7. Loss of *Crk* and *Crkl* in the endocardial lineage does not affect the expression of major proteoglycans.
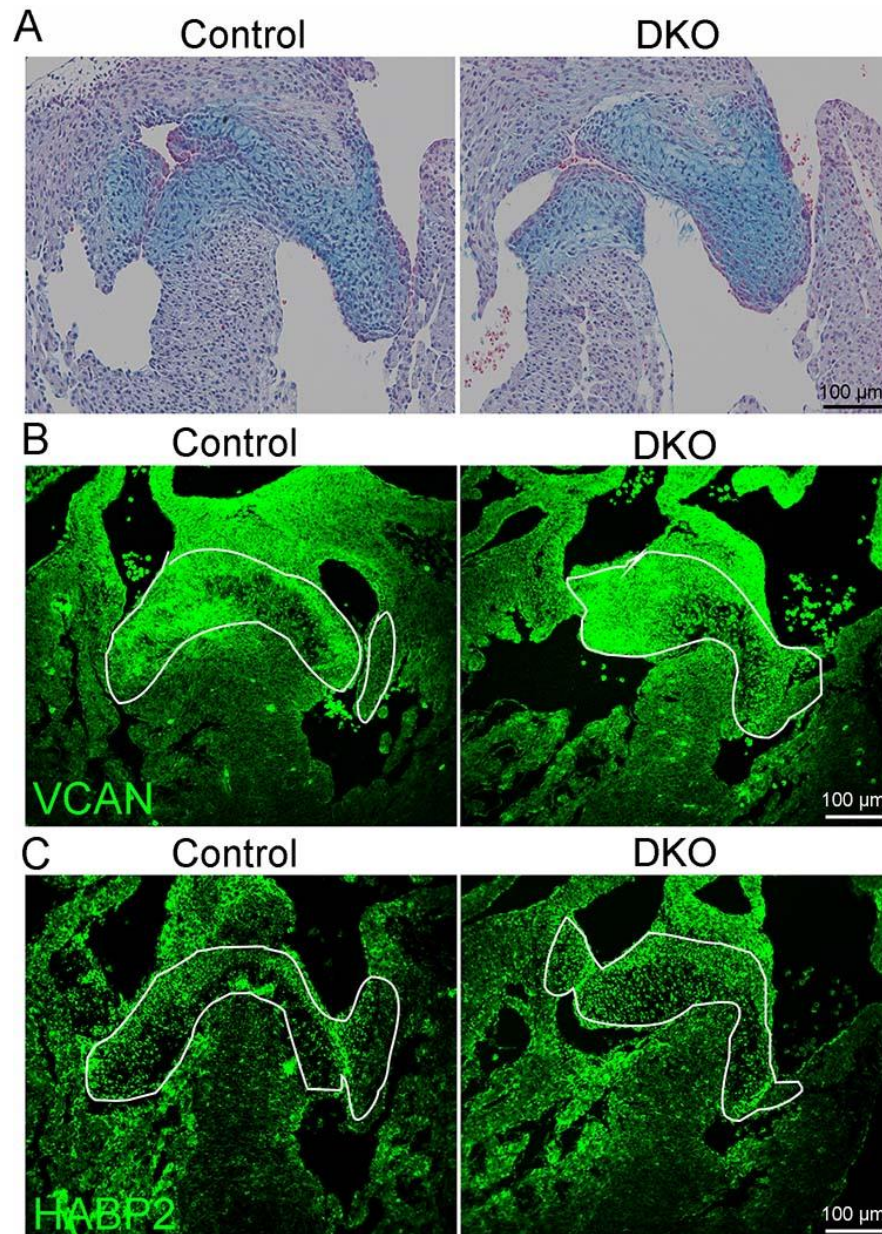
A, Representative images of Alcian Blue staining showing a comparable level of proteoglycans in the remodeling atrioventricular valves of E13.5 control and DKO embryos. **B** and **C,** Representative immunostaining images showing a comparable level of VCAN (**B**) and HABP2 (**C**) in the remodeling atrioventricular valves of E13.5 control and DKO embryos. DKO, *Crk* and *Crkl* double knockout.

Figure S8. Loss of Crk and Crkl reduces ERK signaling.

Representative images of immunostaining showing the protein level of pERK1/2 and pSMAD1/5/9 in the remodeling atrioventricular valves of E13.5 control and DKO hearts. The fluorescence intensity was quantified. n=4/group. Unpaired Student's t-Test was used for statistical calculation. Δ *p*<0.01. DKO, *Crk* and *Crkl* double knockout.